

Spaces and sequences in the hippocampus: a homological perspective

A. Babichev, V. Vashin¹, Y. Dabaghian¹

¹*Department of Neurology,
The University of Texas McGovern Medical School,
6431 Fannin St, Houston, TX 77030
*e-mail: Yuri.A.Dabaghian@uth.tmc.edu
(Dated: February 19, 2025)*

Topological techniques have become a popular tool for studying information flows in neural networks. In particular, simplicial homology theory is used to analyze how cognitive representations of space emerge from large conglomerates of independent neuronal contributions. Meanwhile, a growing number of studies suggest that many cognitive functions are sustained by serial patterns of activity. Here, we investigate stashes of such patterns using *path homology theory*—an impartial, universal approach that does not require *a priori* assumptions about the sequences' nature, functionality, underlying mechanisms, or other contexts.

We focus on the hippocampus—a key enabler of learning and memory in mammalian brains—and quantify the ordinal arrangement of its activity similarly to how its topology has previously been studied in terms of simplicial homologies. The results reveal that the vast majority of sequences produced during spatial navigation are structurally equivalent to one another. Only a few classes of distinct sequences form an ordinal schema of serial activity that remains stable as the pool of sequences consolidates. Importantly, the structure of both maps is upheld by combinations of short sequences, suggesting that brief activity motifs dominate physiological computations.

This ordinal organization emerges and stabilizes on timescales characteristic of spatial learning, displaying similar dynamics. Yet, the ordinal maps generally do not reflect topological affinities—spatial and sequential analyses address qualitatively different aspects of spike flows, representing two complementary formats of information processing.

I. INTRODUCTION

One of the central tasks in neuroscience is to explain learning and memory through neuronal activity [1]. A key role in enabling these phenomena is played by the hippocampus—one of the brain’s fundamental regions, both functionally and phylogenetically. Broadly, there are currently two perspectives on the organization of hippocampal neuronal activity. On the one hand, it is believed that memory episodes may be encoded and invoked by the firings of individual cells and their combinations, known as *cell assemblies*¹.

Specifically, hippocampal neurons, called place cells, learn to activate in specific areas within an environment—their respective place fields. Subsequent firings of these cells may be triggered not only by the animal’s physical visits to these fields but also by the recall of previous visits or anticipation of upcoming ones [2–5]. Suppressing the firing of select place cells using electrophysiological or optogenetic tools can prevent the animal from entering corresponding fields, whereas their stimulation can prompt such visits [6, 7]. Curiously, hippocampal cells may also learn to selectively respond to odors, visual cues, objects, memory episodes, and more, thus mapping out not only spatial but also mnemonic information [8–12].

On the other hand, the hippocampus also enables animals to understand event sequences, plan series of actions, learn cue sequences, and more [13–15]. For instance, rats with hippocampal lesions can recognize odors but struggle to memorize their order [13]; lesioned monkeys have difficulty learning new sequences of stimuli [13, 16]; and humans with hippocampal damage lose the ability to rank the positions of objects in learned sequences [17–20]. Physiologically, sequential learning and recall are believed to be enabled by a series of consecutively firing cells and their assemblies, and hence the temporal order of activity receives significant attention [21–24].

The mechanisms that produce either ordinal or spatial cognitive maps—and the principles that allow the hippocampus to sustain both functions—remain unknown. Generally, it can be argued that hippocampal representations are coarse, providing a rough-and-ready framework—with great computational speed, flexibility and stability—into which geometric details, supplied by other brain regions, could be situated over time [25]. For example, memorized sequences can scale to accommodate different physical sizes and temporal durations, adapting to specific tasks or environments [26–28]. Moreover, this scaling can be modulated by cognitive and behavioral circumstances; for instance, items may be subjectively judged as “closer” or “farther” apart, depending on the context [29]. Similarly, hippocampal cells preserve their relative order of spiking amidst gradual geometric transformations of the navigated environment [30–36], which also points at a qualitative, topological nature of the encoded map [36–38].

Over the last decade, several topological approaches have been used to model hippocampal maps and their dynamics, based on simplicial [39], persistent [40–48], and zigzag [49, 50] homology theories, along with other techniques [51, 52]. However, in all these cases, constructing cognitive maps were viewed as assembling contributions from individual spiking units, rather than building frameworks of sequential activity. To address the latter, we utilize an alternative technique—path homology theory [53–57], which qualitatively broadens the topological perspective on hippocampal activity.

The paper is organized as follows. Section II discusses current topological models of hippocampal activity and outlines path homology theory along with its connections to physiology. The results of path-homological analyses of simulated neuronal dynamics are presented in Section III and discussed in Section IV.

¹ Throughout the text, semantic highlights and terminological definitions are given in *italics*. Key mathematical terms are defined in Sec. VI

II. TOPOLOGICAL METHODS

A. Simplicial schema of cognitive map

A cell assembly is a transient group of neurons that work together² to elicit responses from downstream “readout” neurons [24]. A given neuron, c_i , may participate in multiple assemblies, meaning the cell assemblies are interconnected. Formally, an assembly can be viewed as an abstract simplex (Fig.1A),

$$\sigma_i \equiv [c_{i_0}, c_{i_1}, \dots, c_{i_k}] \equiv \sigma_{i_0 i_1 \dots i_k}, \quad (1)$$

with the subsimplexes corresponding to independently activating “subassemblies” of σ_i [59–61]. The combinations of cells activated by time t form a simplicial coactivity complex,

$$\mathcal{T}(t) = \cup_{t_i < t} \sigma_i, \quad (2)$$

which provides a collective representation of the information encoded by individual spiking units [47]. The shape of the coactivity complex reflects the overall, large-scale structure of information and exhibits properties manifesting at the cognitive level. For instance, such complexes capture the shape of the navigated environment: temporally filtered persistent simplicial homologies of $\mathcal{T}(t)$ evolve to match the homological structure of the environment, $H_*(\mathcal{T}(t)) = H_*(\mathcal{E})$, $t > T_{\min}$ (for terminological definitions, see Sec.VI). The minimum time required for this process, T_{\min} , approximates the physiological *learning time* [38, 41–48].

Second, using a simplicial schema to describe neuronal activity aids in interpreting neurophysiological computations. For example, the assemblies igniting along a navigated path, γ , induce a series of consecutively activating simplexes that form a representation of γ —a simplicial trajectory,

$$\Gamma = \{\sigma_1, \sigma_2, \dots, \sigma_n\}, \quad (3)$$

embedded in \mathcal{T} . Such trajectories not only represent ongoing behavior [62–64], but they also enable the reconstruction of an animal’s past navigational experiences and the prediction of upcoming, planned journeys [13]. Even the possibility of associating neuronal spiking with place fields relies on the topology of the coactivity complex [65, 66].

The structure of simplicial complexes is derived from the adjacencies of their simplexes. Algorithmically, this is achieved by introducing an operator, ∂ , which splits the boundary of each simplex (1) into facets, as illustrated in Fig. 1B,

$$\partial\sigma_{i_0 \dots i_k} = \sum_{l=0}^k (-1)^l \sigma_{i_0 \dots \cancel{i_l} \dots i_k}, \quad (4)$$

where the crossed-out index i_l denotes the omitted vertex v_{i_l} [59–61]. The key objects in the theory are simplex chains—arbitrary collections of simplexes that span the complex and collectively capture its shape. For instance, simplicial trajectories (3) can be viewed as contiguous chains of abutting simplexes.

If a simplicial chain borders a simplex of higher dimensionality, its segments can be “snapped over” the boundary of that simplex, producing a chain deformation (Fig.1D). Correspondingly, if two chains, c_1 and c_2 , can be deformed into one another—that is, if they differ by a collection of full boundaries—they may be considered equivalent, or homologous (Sec.VI). Simplicial topology

² “...much like jazz musicians” [58].

exploits the phenomenon that sets of homologous cycles correspond to elements of the complex’s topological structure, such as holes, cavities, pieces, tunnels, and so forth [59–61]. Specifically, classes of equivalent simplicial trajectories (3) in representable coactivity complexes mirror the structure of the environment covered by the place fields, including areas, obstacles encircled by the rat, and potential shortcuts the rat can take [38, 41–43].

Algebraically, sets of homologous chains form abelian groups or vector spaces, depending on the coefficients used to count the simplexes. With coefficients from an algebraic field, \mathbb{K} , one obtains n vector spaces, one for each dimension: $H_0(\mathcal{T}, \mathbb{K}), H_1(\mathcal{T}, \mathbb{K}), \dots, H_n(\mathcal{T}, \mathbb{K})$, commonly referred to as the simplicial homologies of \mathcal{T} . The dimensionalities of these homology spaces, $b_k = \dim(H_k(X, \mathbb{K}))$, known as Betti numbers, count connectivity components (β_0), holes and tunnels (β_1), cavities (β_2), and so on. In this study, we use the binary field, $\mathbb{K} = \mathbb{Z}_2 = \{0, 1\}$, which is used without explicit reference.

In practice, the hippocampal coactivity complex is often constructed as the clique complex associated with the graph of coactivity, \mathcal{G} , also known as the cognitive graph [67–73]. The nodes of this graph correspond to principal cells, and its links represent either physiological or functional connections between them. If these connections are directed (e.g., extending from presynaptic to postsynaptic cells), the graph is directed and referred to as a *digraph*. Otherwise, if the connections represent undirected coupling, such as the rate of coactivity between cells, the coactivity graph is undirected.

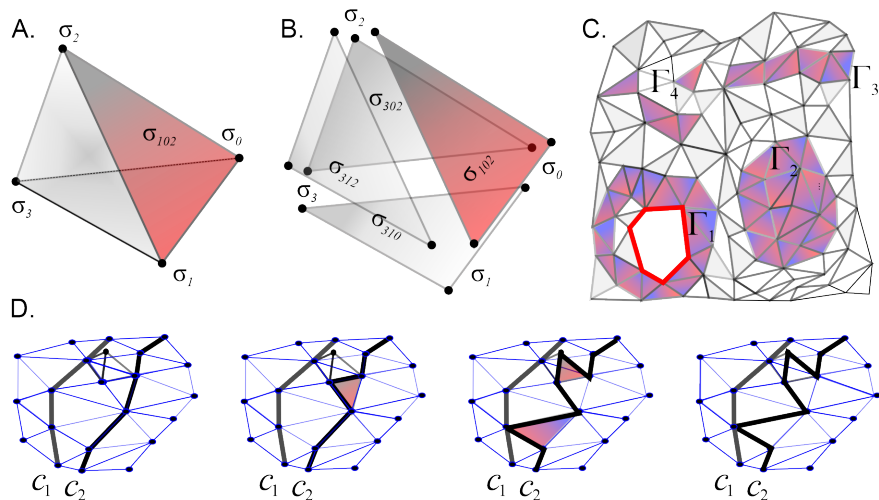


FIG. 1. Simplexes and simplicial chains. **A.** Simplexes are k -dimensional polytopes spanned by $k + 1$ vertices. Shown is a three-dimensional (3D) simplex—a tetrahedron. **B.** The boundary of a 3D simplex is a combination of its two-dimensional (2D) facets. **C.** Simplexes with matching boundaries form a simplicial complex. A chain in such a complex is an arbitrary combination of simplexes, counted with coefficients from a field \mathbb{K} . Here colored simplexes illustrate 2D chains connected ($\Gamma_1, \Gamma_2, \Gamma_3$) and disconnected (Γ_4), contractible ($\Gamma_2, \Gamma_3, \Gamma_4$) and topologically nontrivial—a 1D cycle (c_1 , red). **D.** Two homologous one-dimensional (1D) chains, c_1 and c_2 , highlighted by thick black lines. The panels show a series of discrete deformations that transform one chain into the other, produced by “snapping” segments of c_2 over the boundaries of adjacent (red) simplexes.

In applications, specific constructions of cliques may be used to capture different physiological phenomena. For instance, cliques formed over time from frequently co-occurring lower-order coactivities (e.g., pairs or triples of cells) can model input-integrating cell assemblies, whereas large groups of simultaneously co-firing cells can represent coincidence-detecting cell assemblies. Both mechanisms have been experimentally identified, making the corresponding coactivity complexes viable functional representations of physiological coactivity pattern [41–48].

B. Sequential schema of neuronal activity

If ordered sequences of neurons’ firings, rather than nearly-independently igniting cell groups, serve as functional units of neuronal activity, then the approach described above requires principal modifications. Let us represent the population of active units (cells or their assemblies) by a set of vertexes, $V = \{v_1, v_2, \dots, v_n\}$, and consider sequences of various lengths,

$$e_i = \{v_{i_0}, v_{i_1}, \dots, v_{i_k}\} \equiv e_{i_0 i_1 \dots i_k}. \quad (5)$$

Following the terminology of path homology theory, we will also refer to (5) as an *elementary path* running through the set V [53, 54]. A simplicial path (3) is one example of an elementary path comprised of igniting cell assemblies, while a sequence of individual neurons activated autonomously in the animal’s brain (e.g., during sleep) is another [74–76]. Note that, since the firing units in (5) spike in order at times $t_{i_0} < t_{i_1} < \dots < t_{i_k}$, each sequence (5) is characterized by a specific start and completion time. The set of spiking sequences produced by a particular moment t then forms a *path complex*,

$$\mathcal{P}(t) = \cup_{t_i < t} e_{i_0 i_1 \dots i_k}, \quad (6)$$

which is a path analogue of $\mathcal{T}(t)$ (Fig. 2A). The only requirement for the collection of paths (6) is that if a path e_i is included, then the paths obtained by “plucking” the ends of e_i must also belong to $\mathcal{P}(t)$ (Fig. 2B). In other words, given a cell sequence (5), its shorter contiguous subsequences are assumed to contribute to the informational framework encoded by $\mathcal{P}(t)$ —a physiologically natural assumption.

Note that building a path complex, e.g., constructing a path complex from a dataset of spiking series, requires specifying all elementary paths: the existence or absence of paths should not be presumed. However, if sequences follow a particular grammar, it may be possible to identify a specific “template” that generates them [75–77]. For instance, if a complex \mathcal{P} contains paths assembled from specific pairs of vertices, then \mathcal{P} can be induced by traversing a certain graph G , where these selected pairs are connected by edges [53, 54]. In such a case, given a finite set of observed paths, one may assume that the observations are partial, while the “ultimate” path complex encompasses all paths consistent with the graph’s connectivity. This allows for the study of the pool of all possible vertex sequences. Physiologically, such a graph may emerge, e.g., as the synaptic configuration of the underlying network, or as a coactivity graph, \mathcal{G} [77]. In the following sections, we will focus on these *graph-representable* path complexes, although the theory allows for more general constructions.

The homological description of path complexes develops similarly to simplicial homology theory. Viewing an elementary path (5) of length k as analogous to a k -dimensional simplex, one can construct its “structural boundary” as the formal alternating sum,

$$\partial e_{i_0 \dots i_k} = \sum_{l=0}^k (-1)^l e_{i_0 \dots \cancel{i_l} \dots i_k}, \quad (7)$$

where $e_{i_0 \dots \cancel{i_l} \dots i_k}$ runs from v_{i_0} to v_{i_k} , omitting the vertex v_{i_l} (Fig. 2C). Thus, the “boundary” of a path of length k is a combination of its $(k + 1)$ subpaths, each of length $k - 1$.

The next step is to consider *path chains*—arbitrary combinations of elementary paths—and to view two chains as homologous to one another if their difference is the boundary of another path chain, in the sense of formula (7) [53, 54]. The resulting equivalence classes, properly counted, form vector spaces called the *path homologies* of a path complex \mathcal{P} , denoted below as

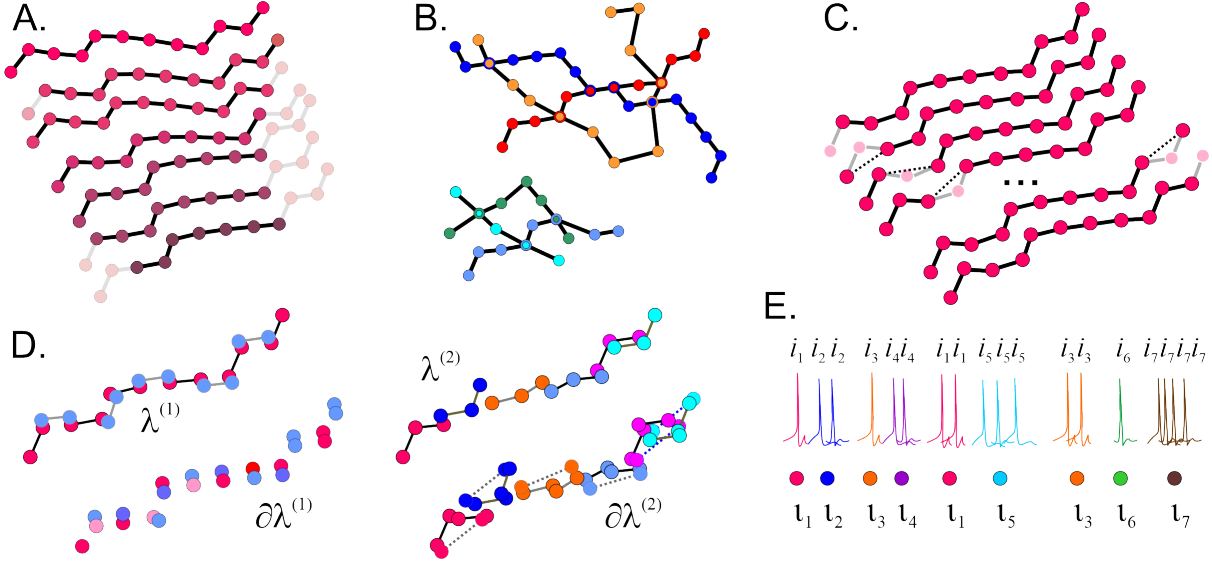


FIG. 2. Path, path chains, path complexes. **A.** An elementary path e of length 12 and examples of shorter paths obtained by ‘plucking’ its end vertices. All truncated paths must be included into each path complex that contains e . **B.** A path complex with two-components and six maximal elementary paths. Presence of the subpaths obtained by “plucking” the longest paths is implied. **C.** The path-boundary (7) of the sequence e illustrated on the top of panel A. Note that only the first and the last paths shown on this panel also appear on panel A. **D.** A sequence of k elements can be viewed as combination of pairwise links (length-one path chain, $\lambda^{(1)}$, left panel), or triples of consecutive vertices (length-two path chain, $\lambda^{(2)}$, right panel), etc. The boundaries of such chains, $\partial\lambda^{(1)}$ and $\partial\lambda^{(2)}$, are shown below. **E.** A collection of bursting neurons, t_1, t_2, \dots, t_7 , produce series of spikes marked by repeating indexes, i_k : neuron t_2 yields two spikes in a burst, neuron t_5 yields three spikes, neuron t_7 yields four. Regularized sequence reveals the order in which the neurons fire (bottom).

$HP_0(\mathcal{P}), HP_1(\mathcal{P}), \dots$, which describe its structure just as simplicial homologies describe simplicial complexes.

This outline requires several stipulations. First, unlike the subsimplexes on the right-hand side of (4), which architecturally belong to $\mathcal{T}(t)$, the “path-facets” on the right-hand side of (7) may not fit the path complex, meaning that formula (7) may be ill-defined. For example, consider a path complex \mathcal{P}_e that contains a single linear path (5) and its required “truncations.” In this case, formula (7) generates subpaths that skip intermediate vertices and therefore do not belong to \mathcal{P}_e (Fig. 2C).

This perplexity is resolvable (see below) and even desirable: if paths responded to the boundary operator (7) in the same way that simplexes respond to the boundary decomposition (4), the two homology theories would simply emulate one another. Instead, the principles for identifying structurally equivalent serial patterns of activity are genuinely different from simplicial equivalence, pointing to qualitatively distinct organizations of information.

Of course, paths that behave like simplexes do exist, but they are non-generic and consist only of those that traverse simplex vertices. A complex \mathcal{P} comprised exclusively of such “folded-into-a-simplex” paths, which contain *all* boundary subpaths of *all* of its elementary paths, is structurally similar to a simplicial complex and is referred to as perfect in [53–56]. However, most path complexes are far from perfect; that is, boundary subpaths of most of their elementary paths are missing, resulting in path homologies that differ substantially from the simplicial homologies of the underlying graph’s clique complex.

The second point is that there are multiple ways to interpret a given firing series as a path. A string of k vertices can be viewed not only as a single path of length k , but also as a combination of 1-vertex paths—individual nodes (a 0-chain, $\lambda^{(0)}$), a collection of 2-vertex paths (a 1-chain of graph links, $\lambda^{(1)}$), or as sequences of 3-vertex paths, *i.e.*, link pairs (a 2-chain, $\lambda^{(2)}$), link triples (a 3-chain, $\lambda^{(3)}$), and so on, with all shorter constituents overlapping in arbitrary ways (Fig. 2D). As it turns out, reasoning in terms of such “path chains,” rather than individual paths, allows for rectifying the unencumbered boundary operator (7) and transforms any collection of paths into a self-contained complex [53–56].

Third, paths that repeatedly traverse the same vertices, such as $e_{i_1 i_2 i_2 i_3 i_3 i_4 i_4 i_1 i_1 i_3 i_3 i_5 \dots}$, are possible but often redundant in practical analyses. For example, consider a complex where the elementary paths correspond to sequences of spikes, each indexed by the neuron that produced it. Since neurons tend to “burst,” firing spikes in rapid succession, such paths will contain multiple repeating indices (Fig. 2E, [78, 79]). In analyses focusing on the order of neuron activation, these repetitions are uninformative and should be factored out. Conveniently, path homology theory allows for the exclusion of index repetitions by reducing each path to its unique *regular representative* with distinct consecutive vertices [53, 54]. At the graph level, this corresponds to removing trivial loops, e_{ii} . The resulting paths form *regular path complexes*, described by *regular path homologies*. Below we consider only these regular path complexes and omit the term “regular” (see Sec. VI).

With these provisions, path homologies provide a natural, context-independent description of serial activity pools, and, together with simplicial homologies highlight principles by which neuronal activity may be organized. In the following sections, we explore this question by simulating the simplicial complexes of coactivity and the complexes of firing sequences produced by the hippocampus during spatial navigation. We then evaluate their spatial and ordinal structure and discuss certain physiological implications of their homological classification.

III. RESULTS

We simulated the rat’s movement in a small, low-dimensional enclosure covered by randomly scattered place fields (Fig. 3A). From the resulting spiking patterns, we constructed the coactivity graph, \mathcal{G} , by identifying pairs of frequently cofiring cells [38, 41, 42, 67]. The corresponding coactivity complex is dynamic (Fig. 3B): in the early stages of navigation, when only a few cell groups had a chance to cofire, \mathcal{T} is small, fragmented, and contains numerous holes, cavities, tunnels, and other features, most of which lack physical counterparts. When the spiking parameters are biologically realistic, these “spurious” structures tend to disappear as the pool of coactivities grows (Fig. 3C). Consequently, the complex \mathcal{T} becomes representable and takes on the topological shape of the surrounding environment [65].

In other words, as spiking accumulates, the pool of homologous simplicial chains consolidates, revealing the topological structure of the underlying space (Fig. 3B) [38, 41–48], which is reflected in the animal’s spatial behavior [80–86].

On the other hand, the very same process can be interpreted as the formation of a path complex of simplicial trajectories. Indeed, the simplicial complex \mathcal{T} may be viewed as one or several “folded” simplicial paths: the assemblies that ignite at the animal’s current position produce active simplexes at the “tip” of an unfolding simplicial path Γ , while the simplexes left behind in its “tail” accumulate into \mathcal{T} .

Furthermore, at each moment of its development, $\mathcal{T}(t)$ can be represented by the maximal simplex connectivity graph, $\mathcal{G}_{\mathcal{T}}(t)$, whose vertices correspond to the cell assemblies—the maximal simplexes $\sigma_i \in \mathcal{T}(t)$ —connected by an edge e_{ij} if σ_i overlaps with σ_j . The simplicial paths Γ then

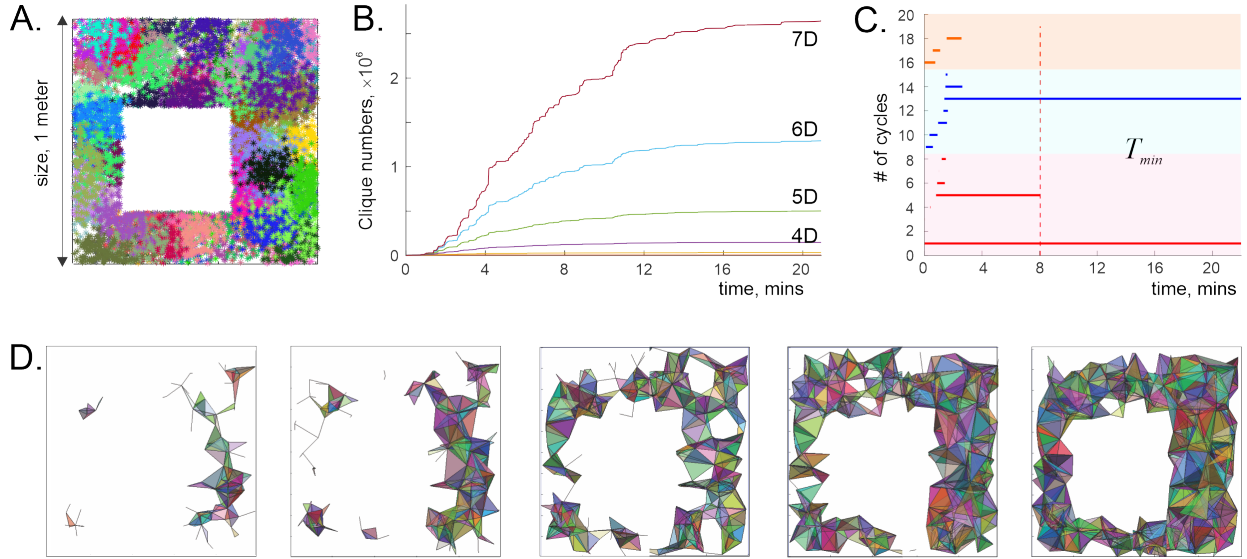


FIG. 3. Simplicial dynamics. **A.** 2D arena with one hole, $\mathcal{E}_1^{(2)}$, sized $1m \times 1m$, typical for electrophysiological experiments [89, 90], covered by 200 simulated place fields. The cells fired in the order their fields were traversed. Each dot of a particular color represents a spike fired by the corresponding cell at that location. Each cluster of colored dots represents a place field. **B.** As the animal navigates, the set of cells that have spiked grows, as does the pool of coactive cell combinations. Shown is the growing population of seven-dimensional (7D), six-dimensional (6D), five-dimensional (5D), *etc.*, cliques of \mathcal{G} , *i.e.*, simplexes of $\mathcal{T}(\mathcal{G})$. **C.** The corresponding topological evolution of the coactivity complex: at first, \mathcal{T} is small and fragmented, but as the complex grows in size, its structure simplifies. Top, orange streaks mark the timelines of the noncontractible 2D cavities, middle, blue timelines pertain to 1D holes and the bottom, red timelines follow 0D loops—pieces of \mathcal{T} . From early on, higher-dimensional Betti numbers, $b_{D \geq 2}$, are suppressed, allowing representability of the complex [65]. The spurious holes close up by $T_{\min} = 3.2$ min, and complex fuses into one piece in about 8.0 mins, at which point \mathcal{T} becomes topologically equivalent to $\mathcal{E}_1^{(2)}$. **D.** Pictorial dynamics of the coactivity complex, with 2D facets projected into the navigated environment.

correspond to sequences of edges in $\mathfrak{G}_{\mathcal{T}}$. In the spirit of the persistence approach [87, 88], the path homologies of this maturing graph reveal, moment by moment, how the ordinal structure of igniting cell assembly series unfolds over time. This represents a new kind of homological dynamic that may also influence the animal’s behavior and cognitive performance.

For the neuronal ensemble illustrated in Fig. 3C, the graph $\mathfrak{G}_{\mathcal{T}}$ initially appears fragmented, as indicated by large values of the path-homological 0th-order Betti numbers, $\beta_0(\mathfrak{G}_{\mathcal{T}}) \sim 8$. This is expected, as the disconnected subgraphs correspond to the connected components of \mathcal{T} ; the 0th order topological loops appear and disappear simultaneously, indicating the consolidation of spatial and ordinal coactivity domains, $\beta_0(\mathcal{T}) = \beta_0(\mathfrak{G}_{\mathcal{T}})$.

On the other hand, first-order homologies, $H_1(\mathcal{T})$ and $HP_1(\mathfrak{G}_{\mathcal{T}})$, may differ significantly from each other. This is because 1D link-chains in \mathcal{T} “cycle” relative to their simplex boundaries (4) differently than the chains of $\mathfrak{G}_{\mathcal{T}}$ edges “cycle” relative to the path boundaries (7). In particular, the high computational cost of evaluating path homologies (Fig.4B) limits the sizes and the densities of the coactivity graphs that can be used in constructing path complexes, *i.e.*, the sizes of spiking populations. Therefore, we restricted our analyses to the series of the most prominently firing cells—those that produce at least four spikes per burst (Fig.2E, [78, 79]).

The results show that the homological dynamics of the emerging path complexes, $\mathcal{P}_{\mathfrak{G}}(t)$, share several similarities with the dynamics of the coactivity complex $\mathcal{T}_{\mathcal{G}}(t)$: the population of distinct

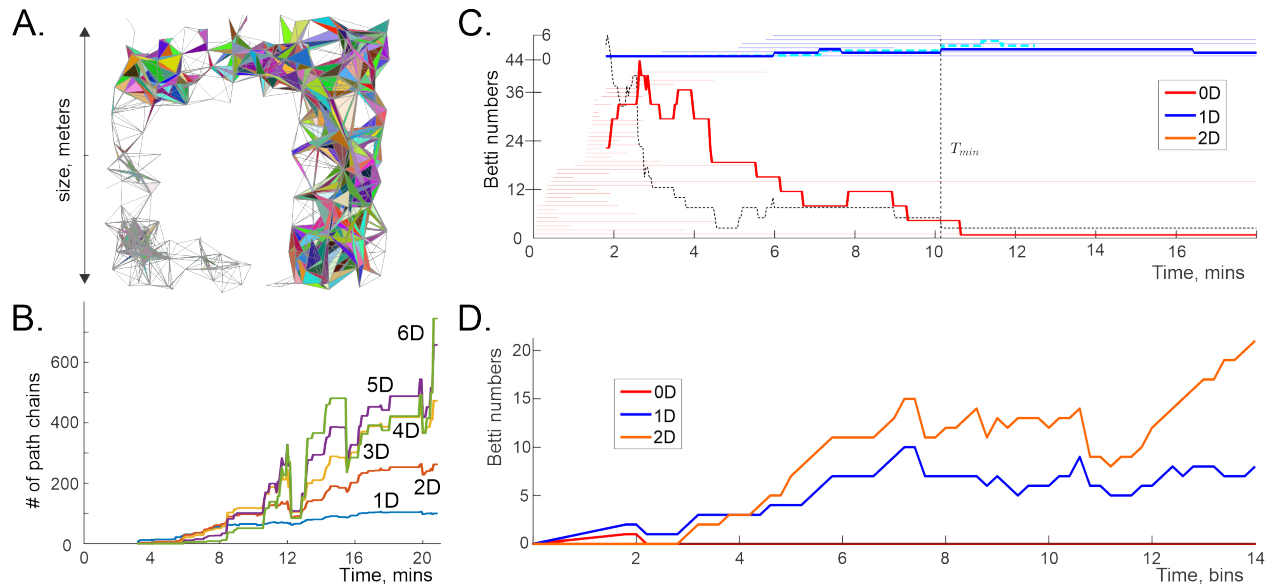


FIG. 4. Temporal dynamics of cell assembly sequences. **A.** Illustrative representation of the coactivity complex’s connectivity graph $\mathfrak{G}_{\mathcal{T}}$ (gray bonds), which defines incidences between the maximal simplexes in $\mathcal{T}_{\mathcal{G}}$ at a particular stage of its development. **B.** The population of 5-vertex, 4-vertex, 3-vertex, ..., path-chains in the path complex $\mathcal{P}_{\mathfrak{G}}$, induced by the maximal simplex connectivity graph $\mathfrak{G}_{\mathcal{T}}$, grows over time. **C.** The path-homological dynamics of $\mathcal{P}_{\mathfrak{G}}$ differ qualitatively, exhibiting similarities with the simplicial-homological dynamics: the number of distinct path-cycles initially increases and then decreases over time. The plot shows the numbers of 0D (blue, β_0), 1D (red, β_1), and 2D (orange, β_2) path-cycles. Higher-order path chains consolidate into a single homology class ($\beta_{k>2} = 0$). The horizontal lines in the background indicate the timelines of spurious topological loops in $\mathcal{T}_{\mathcal{G}}$, identified by simplicial persistent-homological analyses (see Fig. 3C, [38]). **D.** The number of path-homologically distinct path-cycles in a growing random graph (connected, $\beta_0 = 1$) increases, whereas the number of heterologous chains also remains high ($D \gtrsim 6$, not shown).

1D cycles initially increases to high values (with the bursting threshold $n_b \geq 3$), then decreases and stabilizes as distinct serial patterns become path-homologous. This happens over a period $T_{\min}^{(p)}$ that slightly exceeds the simplicial learning time. A similar trend is observed in the population of 2D loops, while higher-order Betti numbers, $\beta_{k>2}$, tend to vanish. The latter indicates that homologically distinct chains composed of long ($k > 3$) elementary paths tend to consolidate. In other words, path-homology analysis suggests that longer sequences of assemblies ignited by traversing firing field maps tend to be homologous to one another, thus capturing less information, whereas collections of shorter sequences form richer structures.

Importantly, this phenomenon is not generic: in our simulations, path-homological Betti numbers of random graphs tend to increase with the graph’s size [91], suggesting that the “homological equalizing” of longer cell assembly sequences may be a property of map-representing graphs.

Adding directionalities to the edges of $\mathfrak{G}_{\mathcal{T}}$, *i.e.*, simulating preferred directions of activity propagation, does not qualitatively alter the previous scenario. The dynamics of β_0 remains unchanged, and β_1 shows exuberant dynamics at the early stages of navigation, which then subsides (longer timescales, with lower intermediate values).

Sequences of neuronal activity traced in most electrophysiological studies follow the connectivity of the original cognitive graph \mathcal{G} , where vertices correspond to individual cells and links represent functional or synaptic connections between them. This graph is typically sparser than

$\mathcal{G}_{\mathcal{T}}$, which relaxes the numerical restrictions on firing activity. We simulated the development of this graph during the rat’s running session discussed above (Fig. 3A), focusing on cells that produced at least three spikes per burst (Fig. 5A). The resulting path-homological dynamics exhibited familiar characteristics: initially, \mathcal{G} induces many spurious, heterologous sequences, which is followed by a period of consolidation and stabilization (Fig. 5B).

The fact that this period aligns closely with the cell assembly sequence learning timescale suggests that information encoded by both the neuronal and cell assembly sequences becomes accessible over similar timeframes. Additionally, the number of homologically distinct, closed neuronal firing sequences is comparable to the number of heterologous cell assembly path cycles and the number of simplicial loops in \mathcal{T} (Figs. 3, 4). If the connectivity graph is directed, reflecting, *e.g.*, the synaptic connections between neurons, then the intermediate population of nonidentical short sequences is higher (β_1 and β_2 grow), but the overall path-homological dynamics remains similar.

In a 3D environment, the connectivity graphs induced from the place field maps produce a population of homologically distinct 2D path-loops, in both vertex (neurons) and clique (cell assembly) sequences, that persist through the simulated period. To obtain these results, we simulated moves through a 3D topological cylinder over the 2D environment shown on Fig. 3A, $\mathcal{E}_1^{(3)} = \mathcal{E}_1^{(2)} \times I$, where $I = [0, L]$ is a Euclidean interval (Fig. 5C). The size of the base and the height, L , were scaled to match the proportions of a bat’s cave described in [92], about 3 meters across [43]. The resulting space has the same fundamental group, $\pi_1(\mathcal{E}_1^{(3)}) = \pi_1(\mathcal{E}_1^{(2)}) = \mathbb{Z}$, and the same topological complexity [93, 94], and therefore poses a comparable topological learning task as its 2D counterpart. The lengthening of the path-homologically nontrivial spiking chains may hence be attributed to the increase of the underlying space’s dimensionality (Fig. 5D).

To investigate whether the maximal length of path-homologically distinct sequences,

$$\beta_{\max} = \max_{k,t}(\{\beta_k(t) > 0\}), \quad (8)$$

and its duration, $|T|$, where

$$T = \{t : \max_k \beta_k(t) = \beta_{\max}\}, \quad (9)$$

continue to increase with the dimensionality of the underlying space, $D = \dim(\mathcal{E})$ —a dynamic also observed in the simplicial homologies of the coactivity complex [65]—we leveraged the fact that all components of our construction (trajectory, place fields, etc.) can be extended to any dimension without affecting the topological complexity or the homotopical and simplicial-homological structure of the space.

Specifically, we constructed several coactivity graphs from the place field maps covering a 4D analogue of the 3D cave (Fig. 5C) and 2D navigational arena (Fig. 3A), $\mathcal{E}_1^{(4)} = \mathcal{E}_1^{(3)} \times I = \mathcal{E}_1^{(2)} \times I \times I$, and observed that the *path-homological Leray index* (8) increased to $\beta_4 = 3$. The emerging $\beta_D \propto D$ trend in map-induced path complexes (Fig. 5E), as well as the general suppression of higher-order Betti numbers requires further investigations. Biologically, this would imply that longer sequences tend to homogenize, whereas collections of shorter sequences exhibit greater structural richness.

A. Memory spaces

Episodic memory frameworks can be regarded as spaces in which specific memories, m_1, m_2, \dots , correspond to regions, r_1, r_2, \dots [95]. Neurophysiologically, this perspective is instrumental because it allows viewing many cognitive phenomena—such as spatial planning and exploration, transitive and relational inference, memory retrieval, and others—as particular cases of “mental navigation,” thereby facilitating physiological interpretations of data [95–101].

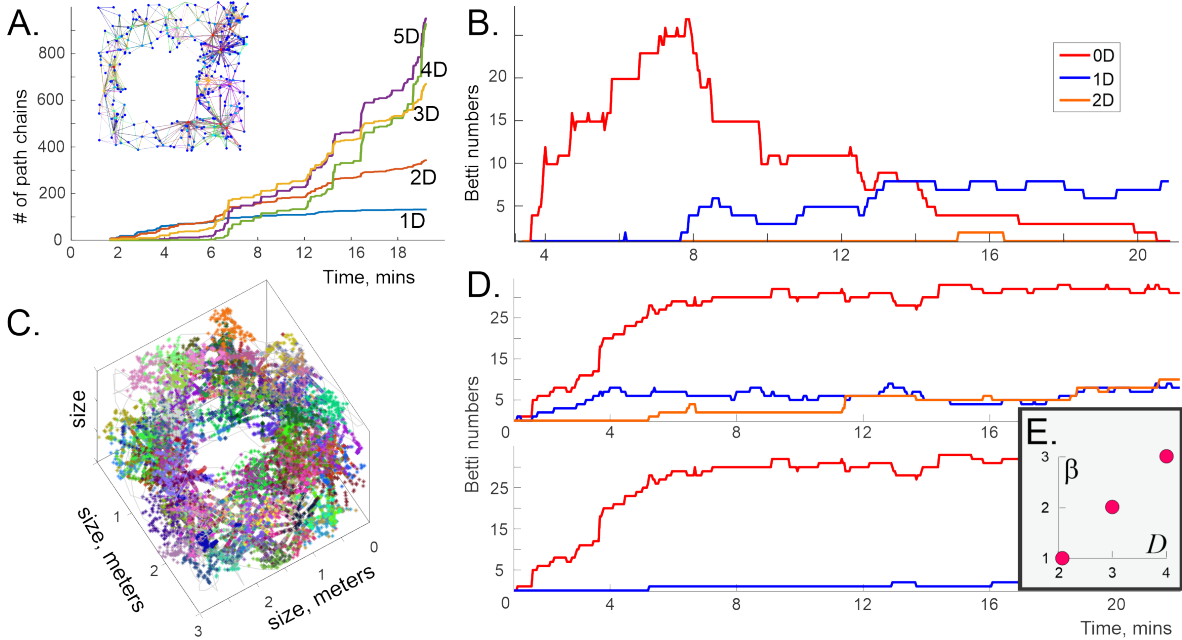


FIG. 5. **Temporal dynamics.** **A.** The population of $5D$, $4D$, $3D$, ... path-chains in the path complex induced by the growing cognitive graph \mathcal{G} (embedded panel) grows with time. **B.** Path-homological dynamics of the coactivity graph \mathcal{G} (neuronal sequences) is consistent with the dynamics of \mathcal{P}_6 (cell assembly sequences): the number of distinct path cycles (Betti numbers β_k) first grows and then decreases with time. Higher-order path cycles vanish. **C.** Place field map in a $3D$ environment with one hole, $\mathcal{E}_1^{(3)}$ (simulated bat movements [43]). Points correspond to spikes fired by a specific cell at a particular location. **D.** $3D$ navigation produces more path-homologically distinct length-0 path cycles, which means that for the select size of place cell ensemble, speed value and the spiking parameters, the coactivity graphs (undirected, top and directed, bottom) have many disconnected components. Note also that the undirected coactivity graph generates a population of persistent, homologically distinct length-2 cycles, which appear only fleetingly in panel B. **E.** Lasting ($|T| \geq T_{\min}$) path-homological Betti-order of the undirected cell assembly connectivity graph grows with the dimensionality of the navigated space.

From a topological standpoint, this interpretation is also natural, as simplicial complexes define finitary spaces: individual simplexes emulate points, x_i (“memory nodes”), and their agglomerates represent broader memory scopes, r_i . Essentially, this construction extends the cell assembly theory [22, 23], which associates cognitive episodes with the activity of cell assemblies. It posits mappings from coactivity simplexes or their complexes to a cognitive map or memory space,

$$f : \sigma_i \rightarrow m_i \in \mathcal{M}.$$

The totality of such mappings defines a *singular coactivity complex* associated with \mathcal{M} , whose homologies determine its topological structure [101].

As mentioned above, a remarkable property of hippocampal coactivity complexes is that they are *representable*, meaning there exists a domain in a low-dimensional Euclidean space, X , covered by a set of regular regions, v_1, v_2, \dots, v_N , whose nonempty overlaps correspond one-to-one with the coactivity simplexes. Specifically, $v_{i_1} \cap v_{i_2} \cap \dots \cap v_{i_k} \neq \emptyset \implies \sigma_{i_1 i_2 \dots i_k} \neq \emptyset$ [65, 66]. As discussed in [65], it is the dimensionality of X that limits the order of non-vanishing Betti numbers, β_s . The experimental discovery of hippocampal representability—the existence of place fields marked a major advance in our understanding of learning, memory, and cognition. In particular, the match between Čech homologies of the place field maps and the simplicial homologies

of the coactivity complex supports interpreting the latter as a discrete topological map of the navigated space [102–104]. Similarly, the match between the simplicial homologies of place cell coactivity and the singular homologies of the corresponding discrete Alexandrov space suggests viewing the latter as a discretized representation of the environment embedded within memory space \mathcal{M} (Fig. 3A) [105–109].

The possibility of describing the ordinal structure of episodic memories by classifying sequences of regions distributed over \mathcal{M} ,

$$\wp = \{r_1, r_2, \dots, r_m\}, \quad (10)$$

opens a complementary avenue for analyses. Structurally, the “topological fabric” of a modeled memory space is defined by the pattern of immediate (minimal) neighborhoods, U_i , of its points, which is described by the *topogenous matrix* [110]:

$$t_{ij} = \begin{cases} 1, & \text{if } x_i \in U_j, \\ 0 & \text{otherwise.} \end{cases} \quad (11)$$

Here, we assume that the memory spaces are T_0 -separable, meaning that different points, $x_i \neq x_j$, have distinct minimal neighborhoods, $U_i \neq U_j$, and we set $t_{ii} = 0$ [105–109]. The matrix (11) can then be viewed as the connectivity matrix of a *topogenous graph* \mathcal{G} , where vertices represent elementary memory nodes and edges define topological overlaps between them.³ The path homologies of the graph \mathcal{G} can thus describe the ordinal organization of memory sequences.

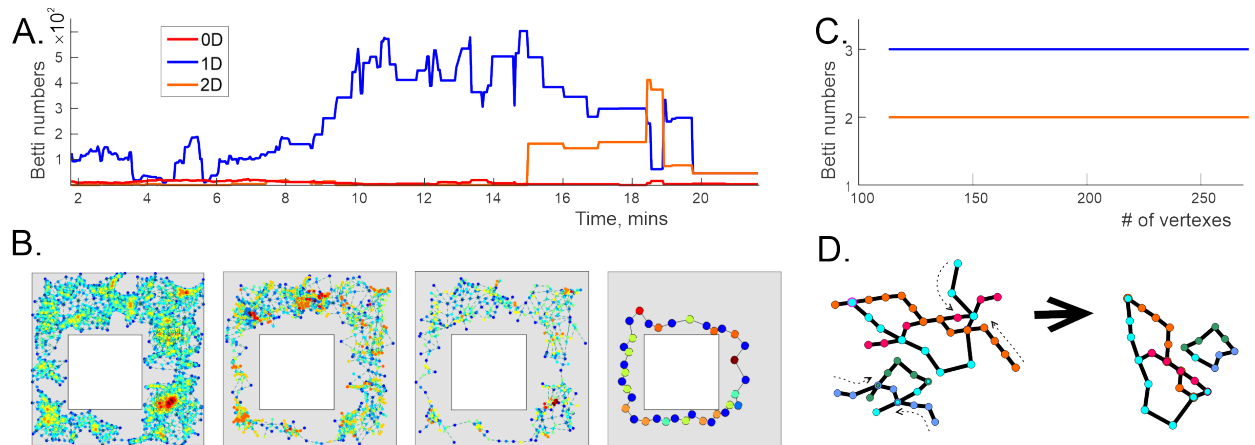


FIG. 6. Temporal dynamics. **A.** Path-Betti numbers for an series of topogenous graphs pertaining to the Alexandrov spaces induced at different stages of the coactivity complex’s development. The topological dynamics, as described by simplicial and singular homologies is identical to the one shown on Fig. 3A. **B.** Elementary locations of the Alexandrov space built for place field map shown on Fig. 3A, and the location maps corresponding to a few of its retractions. The rightmost panel shows the core—maximally reduced schema of the memory space, containing only 36 locations. Color represents the dimensionality of the simplexes giving rise to the points [44, 111]. **C.** Path-homological Betti numbers computed for the topogenous graphs of a retracting Alexandrov space remain unchanged. **D.** An example of a homotopy transformation of two-component graph that eliminates the tentacles. The homotopy of the corresponding path complexes is implied.

³ The graph \mathcal{G} also describes connectivity between all simplexes in the coactivity complex.

We constructed the graph \mathcal{G} for the Alexandrov spaces corresponding to the snapshots of the evolving coactivity complex $\mathcal{T}(t)$, focusing on the most prominently firing cells (at least six spikes per burst period), and traced their path homologies at different stages of the memory spaces’ development. Once again, the dynamics of $\beta_k(\mathcal{G})$ largely mirror those of $\beta_k(\mathcal{G})$ and $\beta_k(\mathcal{G})$, suggesting that the emerging episodic memory chains encoded by place cell activity are structurally similar to cell assembly and neuronal chain order dynamics: disordered at first, then consolidating over the learning period $T_{\min}^{(p)}(\mathcal{G})$.

It is worth noting that the pools of memory sequences could also be analyzed using singular-like homologies, in terms of chains induced by mapping $\hat{\mathcal{G}}_{\mathcal{T}}$ into \mathcal{G} , though we do not pursue this approach here [55].

B. Topological consolidation

As discussed in the Introduction, the hippocampus generates coarse representations of the external world—a “subway map” of memorized experiences [112, 113]. Homological descriptions of this map are even coarser: the network’s structure and spiking dynamics may change significantly without affecting the path or simplicial homologies of the neuronal coactivity complex. For instance, alterations in the simplicial complex \mathcal{T} , such as contractible protrusions, bulges, bends, or overall enlargements or shrinkages (Fig. 3C), remain indiscernible in homological analyses as long as no topological loops are created or eliminated. In other words, homological descriptions reflect only major, qualitative restructurings. Yet physiological changes can be subtler, such as the consolidation of rapidly learned hippocampal memories into longer-term, coarser-grained cortical structures that preserve the spatiality and overall morphology of the original maps [114–120].

The exact physiological mechanisms underlying these processes are unclear, but functionally, they involve eliminating redundant or disused cell assemblies and consolidating inputs from active ones [121, 122]. Phenomenologically, such effects can be modeled by removing structurally redundant simplexes from the coactivity complex \mathcal{T} , reducing the granularity of the corresponding finitary topological spaces while preserving their homologies [57]. In particular, the maximally coarsened memory space—the *core*, $C(\mathcal{M})$ —captures the original topological structure using the smallest number of points and neighborhoods (Fig. 6A) [105–109]. Interestingly, similar compact representations are also discussed in neuroscience as Morris’ “location schemas” [73, 123–125]. In [101], it was argued that such schemas can be constructed as the cores of memory spaces produced by place cells in a given environment, for specific physiological parameters of neuronal activity.

From the path-homological perspective, coarsening a memory space implies a reduction in the associated pool of memory sequences, which could potentially disrupt the overall structure of serial activity. However, direct computations reveal that the path homologies of the “consolidated” set of sequences remain unchanged—that is, a smaller population of heterologous sequences in reduced memory spaces preserve the structure of the original pool (Fig. 6B). In other words, patterns of consolidated activity retain both their ordinal and spatial organization. Biologically, this suggests that serial and spatial frameworks can be consolidated consistently.

Mathematically, the preservation of memory sequences’ homologies results from the fact that spatial reduction amounts to a homotopical transformation of the path complex. By this reasoning, one can use generic graph-homotopy retractions to model the consolidation of the sequential activity framework and the associated decimations of the neuronal population. These transformations, by preserving path homologies, yield a smaller repertoire of spiking activity that retains the original memory structure over smaller memory templates.

For instance, isolated sequences can be contracted to a single node, indicating that, at the level of abstraction used in this approach, solitary series of cognitive events may consolidate into a single episode (Fig.7A,B). Similarly, linear 'tendrils' extending from the graph can be retracted to its base, suggesting that sequences of extraneous cognitive episodes can be integrated into a compact core (Fig.7D). By this reasoning, sequential memory schemas can in general be modeled as retracts of the corresponding coactivity graphs.

IV. DISCUSSION

Representing spiking patterns by simplicial coactivity complexes achieves several objectives. First, it provides a straightforward qualitative model of the cell assembly network—a generic schema that can incorporate numerous cellular-level characteristics and reveal their system-level effects [44, 46, 47, 126]. Second, a coactivity \mathcal{T} can be viewed as the Čech complex associated with the place field map. In morphing environments, where the place field map deforms “elastically” [30–36], its Čech complex remains intact, underscoring the topological aspect of the construction. Third, the simplicial semantics suggests structuring the network activity by identifying equivalent patterns of igniting cell assemblies, interpreting the latter as homologous chains of simplexes. Given the hippocampus’ role in the topological aspect of spatial awareness, such computations may actually occur in the hippocampo-cortical network [80–86].

On the other hand, recent studies portray the hippocampus as a universal generator of firing sequences, which act as functional units for triggering cognitive episodes and behaviors [127–129]. Experimental investigations into sequential neuronal activity reveal familiar patterns: the same firing order can adapt to different spatial and temporal scales, depending on specific tasks, contexts, or environments [26–29]. Consequently, a particular configuration of firing sequences may correspond to a quasi-stable state of the underlying network, and represented by a path complex. The structure of this complex is then derived by an alternative concept of equivalence among its components—path homology.

This approach allows identifying the intrinsic structure of various sequence pools: igniting assemblies, firing cells, and evoked memory episodes—regardless of the underlying physiological mechanisms. The findings suggest, *e.g.*, that hippocampal sequences generated by hundreds of cells and cell assemblies fall into only a few equivalence classes that collectively define the ordinal organization of hippocampal activity. Notably, this organization remains stable across various spatiotemporal scales and is robust to geometric deformations of the environment. It aligns with the retracting coactivity complex, pointing to the possibility of simultaneous consolidation of ordinal and spatial maps [130]. Path-homological analyses further indicate that ordinal structures are predominantly supported by shorter sequences, much like spatial maps rely on the coactivity of smaller cell groups [44, 111], suggesting that biological information is generally conveyed by small computational units. Finally, the ordinal organization of neuronal activity emerges and stabilizes over timescales comparable to those of spatial map learning, exhibiting similar dynamics.

Certain parallels between the simplicial and path-homological approaches are natural, as they ultimately provide complementary descriptions of a unified information flow, share elements, and are functionally interconnected. Indeed, hippocampal maps generally influence the spiking order (much like subway maps define the order in which stations are visited), and, conversely, growing pools of interwoven sequences create nexuses of consistently linked elements that yield connectivity maps (just as traversing enough stations reveals the overall metro plan). Thus, it may appear that the differences between these approaches are merely semantic: if learning is *viewed* as spatial mapping, homologous spiking patterns would be identified “simplicially,” whereas if the focus

is on sequential experiences, like memorizing routes between locations, tracing path homologies among sequenced activities is more appropriate. However, this is not the case—the two principles by which homologous patterns are selected differ fundamentally, leading to qualitatively distinct frameworks: ordinal structures do not generally reflect spatial affinities, and vice versa, and the timescales for establishing these structures also differ. In other words, spatial and ordinal cognitive frameworks are not interchangeable: “mapping out” a new environment is distinct from memorizing routes between locations or internalizing other sequential experiences. Thus, the ongoing “space vs. sequences” debate in the hippocampal literature has a profound mathematical substance [37, 76, 77, 127, 131].

There are many examples of natural scientific systems, deriving their structure and dynamics from homological and cohomological equivalences among their constituents [132, 133]. Similar principle may apply to neuronal systems, where the organization of spiking patterns based on simplicial or path-homological equivalences can be imperative for large-scale, system-level behavior and be manifested at cognitive stage. At this point, it remains *a priori* unclear which homological framework best captures the essence of actual physiological computations—this question must be addressed experimentally. Evidence of nearly simultaneously igniting cell groups [9–12] and intrinsic serial firing motifs [75, 134] suggests that both principles could be implemented within the hippocampus or in supporting networks. In either case, the outlined expansion of qualitative information-processing principles can be seen as a principal generalization of the hypothesized *topological nature of hippocampal activity* proposed in [36–38, 81].

A practical implication of this conjecture is that the well-documented behavioral and cognitive effects produced by topological restructuring of the environment [80–86], should also arise in response to ordinal reorganization. In other words, qualitative changes in the serial organization of the environment, or externally induced alterations in neuronal spiking order, are anticipated to trigger consistent and statistically significant compartmental responses, driven by the necessity to adapt to the change.

A practical implication of this conjecture is that the well-documented behavioral and cognitive effects induced by topological restructuring of the environment [80–86] should also emerge in response to ordinal reorganization. In other words, qualitative changes in the sequential organization of the environment or externally induced alterations in neuronal spiking order should be expected to elicit consistent and statistically significant perceptual and adaptive responses, driven by the necessity to accommodate these changes.

V. ACKNOWLEDGMENTS

We are grateful to Prof. A. Grogor’yan for the software used to compute the path homologies. Additional MATLAB software by Dr. M. Yutin is available SteveHuntsmanBAESystems, see [135].

The work was supported by NSF grant 1901338 and partly by NIH grants R01AG074226 and R01NS110806.

VI. MATHEMATICAL SUPPLEMENT: BASIC NOTIONS AND GLOSSARY

1. Geometric simplexes and complexes

- *Geometric d -dimensional simplex κ^d* is the convex hull of its $(d + 1)$ vertices (Fig. 1A).
- The *facet* opposite to a given vertex in a d -dimensional simplex κ^d is itself a $(d - 1)$ -dimensional simplex κ^{d-1} and vice versa, κ^d can be produced by joining the points of κ^{d-1} to a new, $(d + 1)^{\text{st}}$ vertex (Fig. 1B). The order of vertexes defines the *orientation* of a simplex.
- *Boundary of a d -simplex, $\partial\kappa^d$* , consists of its $(d - 1)$ -dimensional faces (Fig. 1B).

$$\partial\kappa^d = \kappa_1^{d-1} \cup \kappa_2^{d-1} \cup \dots \cup \kappa_{d+1}^{d-1}.$$

- A simplex is *maximal*, if it is not a subsimplex of any other simplex.
- *Geometric simplicial complex K* is a combination of properly assembled geometric simplexes that fit each other vertex-to-vertex, side-to-side, with no overruns or other mismatches (Fig. 1C). Formally, it is required that a non-empty intersection of any two simplexes κ_1, κ_2 in K is another simplex from K .
- The collection of all simplexes of dimensionality d and less forms the *d -skeleton* of a simplicial complex Σ , $sk_d(K)$.

2. Abstract simplexes and complexes

- Since all that matters for quantifying topology of simplicial complexes is how their simplexes match, it is natural to ignore their “filling” altogether and pass on to the notion of *abstract simplexes*—ordered lists of simplexes’ vertexes (1), and their collections—*abstract simplicial complexes*, Σ . An abstract simplex may be intuitively apprehended as the set of vertexes of a geometric simplex. The “face-matching” of the geometric simplexes reduces to the requirement that if an abstract simplex belongs to a simplicial complex, then so do all its faces [59].

3. Graphs

- *Directed graph, or digraph, G* consists of vertices, $V = \{v_1, v_2, \dots, v_n\}$, and directed edges between certain pairs of vertexes. Formally, G is described by its connectivity matrix

$$C_{ij}(G) = \begin{cases} 1, & \text{if } v_i \text{ is connected to } v_j \text{ by edge } e_{ij}, \\ 0 & \text{otherwise.} \end{cases}$$

If the matrix C_{ij} is symmetric, the graph is viewed as undirected, *i.e.*, e_{ji} always exists if e_{ij} does.

- Any graph is a 1D simplicial complex.
- *Digraph map $f : G \rightarrow H$* sends vertexes v_i of the digraph G into the vertexes w_p of the digraph H , so that each G -edge either maps on a H -edge, or squeezes into a H -vertex. Incidentally, digraphs and maps between them form a category.
- G is *transitive*, if whenever edges e_{ij} and e_{jk} exist, then e_{ik} is also an edge.
- *Line digraph, I_n* , consists of n ordered directed links between consecutive pairs of vertexes, e.g., $I_n = \{v_1 \rightarrow v_2 \leftarrow v_3 \rightarrow \dots \leftarrow v_{n-1} \leftarrow v_n\}$. If the last vertex, v_n , connects to the first, v_1 , then digraph is *cyclic*, e.g., $S_n = \{v_n \rightarrow v_1 \leftarrow v_2 \rightarrow \dots \leftarrow v_{n-1} \rightarrow v_n\}$.
- Linear digraphs of length one are the two *directed dyads*: $I^+ = (v \rightarrow v')$ and $I^- = (v \leftarrow v')$.
- *Cartesian product* of a digraph G with a vertex set V and a digraph H with its vertex set W , is a digraph $G \times H$ whose vertices have a G - and a H -component, (v_i, w_p) . Vertexes (v_i, w_p)

and (v_j, w_q) are connected by an edge if either v_i connects to v_j in G , with the H -component fixed, $w_p = w_q$, or vice versa, w_p connects to w_q in H , with fixed $v_i = v_j$.

- *Cylinder* over a digraph G is the direct product, $G \times I_n$.
- *Clique* of order d , $\zeta^{(d)}$ is a fully interconnected subgraph with $(d + 1)$ vertexes $v_{i_0}, v_{i_1}, \dots, v_{i_d}$.
- *Clique complex* associated with a graph G , Σ_G , is the full collection of G -cliques [136].
- A finite simplicial complex Σ can be represented by the following constructions:
 - i. vertexes of the *simplex connectivity graph*, G_Σ , v_σ , represent simplexes of Σ , connected by an undirected edge $e_{\sigma\sigma'}$ if σ and σ' intersect, $\sigma \cap \sigma' \neq \emptyset$ [136].
 - ii. vertexes v_σ and $v_{\sigma'}$ of the *maximal simplex connectivity graph*, \mathfrak{G}_Σ , are connected by an undirected edge $e_{\sigma\sigma'}$ if the maximal simplexes $\sigma, \sigma' \in \Sigma$ overlap, $\sigma' \cap \sigma \neq \emptyset$.
 - iii. vertexes v_σ and $v_{\sigma'}$ of the *simplex inclusion digraph*, \mathbf{G}_Σ , are connected by a directed edge $e_{\sigma\sigma'}$ if σ' is a facet of σ , i.e., if $\sigma \subsetneq \sigma'$.
 - iv. If Σ is a clique complex, then the *barycentric refinement* of its 1D skeleton, $sk_1(\Sigma) = G$, is the graph whose vertexes correspond to cliques of ζ of Σ , and the edge $e_{\zeta\zeta'}$ between ζ and ζ' exists if $\zeta \subsetneq \zeta'$. Thus, barycentric refinement of G is the connectivity graph of its clique complex Σ_G .
 - v. vertexes v_σ and $v_{\sigma'}$ of the *face connectivity digraph*, \mathbf{G}_Σ , connect by $e_{\sigma\sigma'}$ if σ is a maximal facet of σ' , $\dim(\sigma) = \dim(\sigma') + 1$.
 - vi. vertexes v_x and $v_{x'}$ of the *topogenous graph* \mathcal{G}_Σ represent points in a topological space X , and the edges $e_{xx'}$ represent their adjacency.

4. A few bullet points of the simplicial homology theory—for more details see [59–61].

- *Chains* of dimensionality k are formal linear combinations of oriented k -dimensional simplexes, in which σ_1^k is counted m_1 times, σ_2^k is counted m_2 times, etc.,

$$c^k = m_1\sigma_1^k + m_2\sigma_2^k + \dots + m_q\sigma_q^k,$$

with the coefficients from a field \mathbb{K} . If the coefficients come from the Boolean field \mathbb{Z}_2 , then the chain is simply a list of “present” ($m_i = 1$) and “absent” ($m_i = 0$) simplexes. The chains can be added or subtracted from one another, as well as multiplied and divided by coefficients, thus producing linear spaces, $C_k(\Sigma)$. Intuitively, each chain space is an algebraization of its k -dimensional part, e.g., the dimensionality of C_k is given by the number of the k -simplexes in Σ ,

$$\dim C_k = \{\#\sigma \in \Sigma : \dim(\sigma) = k\}.$$

- *Boundary of a k -simplex*, algebro-topologically, is a $(k - 1)$ -dimensional *chain of faces*, as defined by the formula (4). For example, the boundary of an interval σ_{12} oriented from vertex σ_1 to vertex σ_2 is a formal alternated sum $\partial\sigma_{12} = \sigma_1 - \sigma_2$. The boundary of a filled 2D triangle is an alternated sum of its three sides, $\partial\sigma_{012} = \sigma_{12} - \sigma_{02} + \sigma_{01}$, etc.
- *Boundary of a chain* is a combination of the contributing simplexes’ algebraic boundaries,

$$\partial c^k = b^{k-1} = m_1\partial\sigma_1^k + m_2\partial\sigma_2^k + \dots + m_q\partial\sigma_q^k,$$

which is hence an element of the $C_{k-1}(\Sigma)$ -space. The full collection of boundary chains b^{k-1} forms a subspace of $C_{k-1}(\Sigma)$, denoted by $B_{k-1}(\Sigma)$.

- *Nilpotence*. By direct verification, $\partial^2 c^k = 0$, i.e., boundary of a boundary always vanishes.
- *Cycles*. Not all boundaryless chains, $\partial c^k = 0$, are boundaries—in general, they are combinations of simplex chains that “loop onto themselves” in the complex. Such chains are

referred to as *cycles*, and denoted by z . Linear combinations of cycles of dimensionality k also form a vector space, denoted by $Z_k(\Sigma)$, which is smaller than $C_k(\Sigma)$, but generally larger than $B_k(\Sigma)$ [59–61].

- *Chain complex* is a system of spaces C_k , in which higher-order spaces are mapped into lower-order ones,

$$0 \xleftarrow{\partial} C_0 \xleftarrow{\partial} \dots \xleftarrow{\partial} C_{k-1} \xleftarrow{\partial} C_k \xleftarrow{\partial} \dots,$$

as facets of simplexes from C_k embed into C_{k-1} . In other words, at each step the boundary operator ∂ maps C_k into B_{k-1} that lays within C_{k-1} .

- *Homologous chains*. Adding or removing a k -dimensional boundary amounts to deforming a cycle z by “snapping” it over a series of $(k + 1)$ -dimensional simplexes and producing an equivalent, or *homologous* cycle $z \pm \partial c = z'$ (Fig. 1D). Cycles that cannot be matched by adding or removing full boundaries are nonequivalent. Identifying equivalence classes hence amounts to factoring out the “boundary parts,” *i.e.*, taking the quotient of the cycle space by the boundary space, $H_k(\Sigma) = Z_k(\Sigma)/B_k(\Sigma)$. The basis elements of the resulting space of k^{th} *simplicial homology groups*, $H_k(\Sigma)$, represent k -dimensional loops, counted up to a continuous deformation.
- *Betti numbers* are the dimensionalities of homology spaces, $b_k(\Sigma) = \dim H_k(\Sigma)$; these numbers count the topologically distinct k -loops in the complex Σ . For example, deforming a $0D$ chain (a combination of $0D$ points) amounts to “sliding” those points inside of Σ ; the dimensionality of the corresponding homology space (0^{th} Betti number), $\beta_0(\Sigma)$, is equal to the number of “sliding domains” in Σ , *i.e.*, the number of its connected components. If a simplicial complex comes in one piece, its $\beta_0(\Sigma) = 1$. $\beta_1(\Sigma)$ equals to the number of holes in Σ . An example of a $2D$ noncontractible loop captured by β_2 is a “hollow” tetrahedron. Being a topological $2D$ sphere, it can hold no $1D$ loops and hence its Betti numbers are $\beta_0 = 1, \beta_1 = 0, \beta_2 = 1, \beta_{n>2} = 0$.

5. Path homology theory is outlined below following the publications [53–57].

- Let $V = \{v_1, \dots, v_n\}$ a finite set. An *elementary path* of length k is an arbitrary sequence of elements, $e_{i_0 i_1 \dots i_k}$. These paths are basic units of the theory, analogous to simplexes of simplicial topology.
- *Path complex* \mathcal{P} is collection of the elementary paths. Lengths of paths define their order, *i.e.*, correspond to the dimensionality of simplexes. We consider only finite path complexes that include paths up to some maximal length, n . If P_l is the set of all elementary paths of length l , then the collection, $\mathcal{P}_k = P_0 \cup P_1 \cup P_2 \cup \dots \cup P_k$, is the k -skeleton of \mathcal{P} —the analogue of the k -skeleton Σ_k of a simplicial complex.
- The paths forming a complex \mathcal{P} must allow “plucking” of the endpoints, *i.e.*, if $e_{i_0 i_1 \dots i_k}$ is in \mathcal{P} , then $e_{i_1 \dots i_k}$ and $e_{i_0 i_1 \dots i_{k-1}}$ must also belong to \mathcal{P} (Fig. 2B).

6. Algebraization of path chain complexes

- *Path chains* of order k are formal linear combinations of elementary paths of length k , with the coefficients in a field \mathbb{K} ,

$$\lambda = \sum_{i_0 \dots i_k \in V} \lambda^{i_0 \dots i_k} e_{i_0 \dots i_k}.$$

The collection of *all* path k -chains forms a linear space Λ_k , *e.g.*, Λ_0 are linear combinations of vertexes e_i , Λ_1 , are the combinations of all pairs of vertices, e_{ij} , etc.

- *Boundary operator* (7) brakes the elementary paths into segments that precede the q^{th} step and the segments that follow it, *e.g.*, $\partial e_i = e$, $\partial e_{ij} = e_j - e_i$, $\partial e_{ijk} = e_{jk} - e_{ik} + e_{ij}$, etc. By

linearity, the boundary of a generic path chain is

$$\partial\lambda = \sum_{i_0, \dots, i_k} \lambda^{i_0 \dots i_k} \partial e_{i_0 \dots i_k} = \sum_{i_0, \dots, i_k} \sum_{q=0}^k (-1)^q \lambda^{i_0 \dots i_k} e_{i_0 \dots \hat{i}_q \dots i_k}.$$

- By direct verification, $\partial^2\lambda = 0$ for any λ , which implies that the boundary operator (7) induces a chain complex $\Lambda_*(\mathcal{P})$,

$$0 \xleftarrow{\partial} \Lambda_0 \xleftarrow{\partial} \dots \xleftarrow{\partial} \Lambda_{k-1} \xleftarrow{\partial} \Lambda_k \xleftarrow{\partial} \dots,$$

in which the path-chains nullified by ∂ are the path-cycles, $\partial\zeta = 0$ and the chains of the form $\beta = \partial\lambda$ are the boundaries. As with the simplicial complexes, both types of chains form their respective linear spaces, $Z_k(\mathcal{P})$ and $B_k(\mathcal{P})$. The factor space of the path-cycles over the path-boundaries yield the *path homology space*, $HP_k(\mathcal{P})$, analogous to the simplicial homologies of simplicial complexes $H_k(\Sigma)$.

- If a path complex is formed by a collection of certain select, or *allowed* elementary paths, then their linear combinations,

$$A_k(\mathcal{P}) = \left\{ \sum_{j_0 \dots j_k} \alpha^{j_0 \dots j_k} e_{j_0 \dots j_k} \right\},$$

form a subspace of Λ_k . Examples:

- In a graph-representable complex, allowed paths are the ones that run along the graph's edges, other sequence are excluded.
 - The allowed paths on the (maximal) simplex connectivity graph are the sequences of overlapping (maximal) simplexes.
 - From a biological perspective, if V is the full set of cells or assemblies in a given network, the allowed vertexes, P_0 , may be the ones that exhibit activity in a given environment. The allowed links, P_1 , may be the ones that represent synaptic connections, rather than all pairs of coactive cells, P_2 , etc., may be synaptically interconnected triples of neurons, etc.
- In order for the boundary operator (7) to act on A_k , the boundaries of the allowed paths should also be allowed,

$$\partial A_k \subset A_{k-1}.$$

However, in contrast with the simplicial case, where each term in the right hand side of (4) is a part of the complex Σ by design, terms appearing in the right hand sides of (7) may structurally fall out of \mathcal{P} (Fig. 2C). Yet, there exists a subclass of the allowed path chains—the *operational path-chains* that have allowed boundaries,

$$\Omega_k = \{\alpha \in A_k : \partial\alpha \in A_{k-1}\}.$$

A simple, but fundamental property of such paths is that the boundary operator (7) acts on them without fallacies. Indeed, if $\alpha \in \Omega_k$ then $\partial\alpha \in A_{k-1}$, and $\partial^2\alpha = 0 \in A_{k-2}$, which means that $\partial\alpha \in \Omega_{k-1}$. Thus, Ω -paths form their own chain complex, Ω_* ,

$$0 \xleftarrow{\partial} \mathbb{K} \xleftarrow{\partial} \Omega_0 \xleftarrow{\partial} \dots \xleftarrow{\partial} \Omega_{k-1} \xleftarrow{\partial} \Omega_k \xleftarrow{\partial} \Omega_{k+1} \xleftarrow{\partial} \dots,$$

whose homology groups (the *reduced path homology groups* of \mathcal{P}) define the structure of the allowed paths.

- Digraphs and digraph maps form a category, distinct from the category of simplicial complexes and simplicial maps.
- A digraph map $f : G \rightarrow H$ induces a homomorphism of operational chain complexes,

$$f_*|_{\Omega_p(G)} : \Omega_*(G, \mathbb{K}) \rightarrow \Omega_*(H, \mathbb{K}),$$

and of path homology groups,

$$f_* : HP_*(G, \mathbb{K}) \rightarrow HP_*(H, \mathbb{K}).$$

Thus, path homologies can be used to classify digraphs relative to such maps.

7. Simplicial vs. path homologies

- A path complex \mathcal{P} is:
 - perfect*, if it contains all subpaths of its elementary paths, so that $\mathcal{P}_k = A_k(\mathcal{P}) = \Omega_k(\mathcal{P})$. In such complexes, the boundary (7) is structurally identical to (4).
 - monotone*, if its vertices can be numbered such that the numbering increases along each elementary path in \mathcal{P} . In a digraph, this implies that all edges comply with the ordering. For example, if a path complex contains two elementary paths with conflicting vertex order, e.g., e_{i_0, i_3, i_5, i_2} and e_{i_2, i_7, i_5} have a conflicting order of i_2 and i_5 , then this complex clearly can not be monotone. Conversely, any finite complex without such conflicts is monotone.
 - perfect and representable by a digraph if and only if the latter is *transitive*.
- \mathcal{P} is the path complex of a simplicial complex if and only if it is perfect and monotone. This combination is rare in applications, e.g., the neuronal coactivity graph or the synaptic connectivity graph are typically not transitive. To build a positive example, consider elementary paths that pass through vertexes enumerated in increasing order. The subsequences of such paths will also be ordered, *i.e.*, the complex \mathcal{P}_G will be perfect and representable by a transitive graph $G(\Sigma)$, and the homologies $HP_k(G)$ and $H_k(\Sigma)$, $k \geq 0$, will be isomorphic [53, 54].

8. Regularization of path complexes

- *Regular elementary paths* are the ones that contain no consecutively repeating indexes: in $e_{i_0 \dots i_n}$, $i_{k-1} \neq i_k$, for all k . The chain spaces Λ_k can be decomposed into the regular and the irregular components, $\Lambda_k = R_k \oplus I_k$, which, however, do not produce separate path complexes, because R_k and I_k are not, by themselves, invariant with respect to the boundary operator (7). For example, the boundary of a regular path e_{iji} ,

$$\partial e_{iji} = e_{ji} - e_{ii} + e_{ij},$$

includes an irregular segment e_{ii} . It turns out however, that one can build a homological classification of the regular paths simply by discounting “irregularities,” *i.e.*, by viewing two path chains as equivalent, if they differ by an irregular path. In other words, one can use

$$\tilde{\partial} e_{iji} = e_{ji} + e_{ij}$$

instead of the “naïve” ∂e_{iji} above. The resulting equivalence classes contain a unique regular path each, *i.e.*, any path can be reduced to its unique regular representative—*regularized*.

This procedure also induces a regularized boundary operator $\tilde{\partial}$, which allows defining the *regular chain complex*

$$0 \xleftarrow{\tilde{\partial}} R_0 \xleftarrow{\tilde{\partial}} \dots \xleftarrow{\tilde{\partial}} R_{k-1} \xleftarrow{\tilde{\partial}} R_k \xleftarrow{\tilde{\partial}} \dots .$$

whose homologies classify regular paths [53].

- The set of allowed regular k -path is a subset of the total set of regular n -paths. The boundary operator $\tilde{\partial}$ acting on such paths defines regular operational chains,

$$\tilde{\Omega}_k = \{v \in A_k : \partial v \in A_{k-1}\},$$

which are characterized by their regular homologies.

- A path complex \mathcal{P} is *strictly regular* if it is regular and does not breed irregularity, *i.e.*, contains no paths of the form $e_{\dots i j i \dots}$. For example, a path complex of a simplicial complex is strictly regular because its paths' indices are strictly increasing. The path complex of a digraph is strictly regular iff there are no loops (no e_{ii} edges and no simultaneously present e_{ij} and e_{ji} edges). The corresponding homologies are the only ones used in our analyses.

9. Homotopies

- Two digraph maps $f, g : G \rightarrow H$ are *homotopic*, $f \simeq g$, if there is a map $F : G \times I_n \rightarrow H$ such that

$$F|_{G \times \{v_0\}} = f \text{ and } F|_{G \times \{v_n\}} = g.$$

In particular, f and g are one-step homotopic ($n = 1$), $f \simeq g$, if $f(v_i)$ and $g(v_i)$ either connect by an edge or coincide for all v_i .

- Any homotopy, $f \simeq g$, amounts to a finite sequence of one-step homotopies, $(f = f_0) \circ f_1 \circ \dots \circ (f_n = g)$, where $f_0 = id$ is the identity map, and $f_k \simeq f_{k+1}$.
- Two digraphs G and H are *homotopy equivalent*, $H \simeq G$, if there exist digraph maps $f : G \rightarrow H$ and $g : H \rightarrow G$, such that

$$f \circ g \simeq id_H, \quad g \circ f \simeq id_G.$$

The maps f and g are then *homotopy inverses* of each other.

- Homotopy equivalent digraphs have isomorphic path homologies. Homotopic maps induce the *identical* homomorphisms of path homologies.
 - A cylinder over a digraph G is homotopic to its base, $G \times I_n \simeq G$, for any $I_{n \geq 0}$.
 - Natural inclusion of G into a cylinder $G \times I_n$ over it, $i_k : v \rightarrow (v, \iota_k)$, and the projection from a cylinder $G \times I_n$ to its base, $p : (v, \iota_k) \rightarrow v$, induce isomorphism of path homologies.
- *Retraction* of a digraph G onto a subgraph H is a map $f : G \rightarrow H$ that fixes all the vertices of H . A *deformation retraction* is the one that can be homotopically deformed to the identity map. This implies that G and H are homotopically equivalent. Any deformation retraction is a composition of one-step retractions. A one-step retraction is a digraph map that fixes some vertices and moves all others either one step along the edges, or one step against the edges simultaneously.
- A digraph G is *contractible* if it is homotopic to a single vertex. All the homology groups of a contractible graph are trivial, except for $HP_0(G) = \mathbb{K}$ [137].

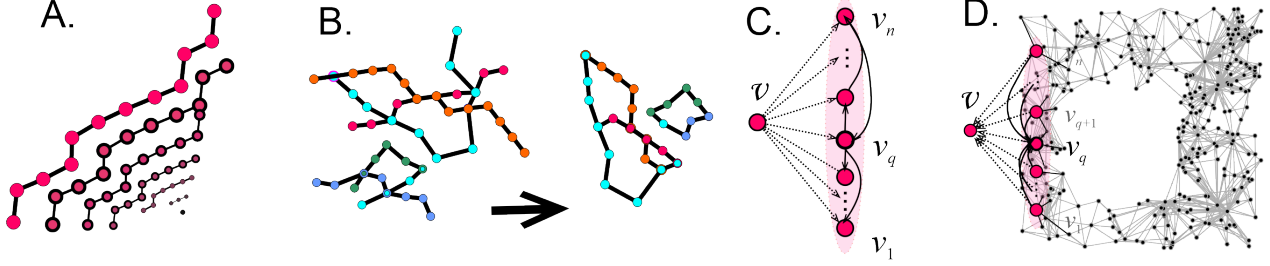


FIG. 7. **Graph homotopies.** **A.** Linear path can be contracted into a single node. **B.** “Tendrils” extending out of generic path complexes can be retracted. **C.** Star graph: if a single “apex” v connects to all other vertexes, v_1, v_2, \dots, v_n , either by outgoing (shown) or by incoming edges, then the entire graph can be contracted to v , *i.e.*, its path homologies vanish. **D.** If a vertex v connects to a set of vertexes v_1, v_2, \dots, v_k , and if one of the latter vertexes, e.g., v_s , connects to the rest of them just as v does (*i.e.*, $e_{v_s v_p}$ exists when $e_{v v_p}$ does and is similarly directed, $p = 1, \dots, k$) then v with all of its adjacent edges can be removed from the graph G without altering its homologies.

- i. A connected tree can be contracted to its root vertex by “trimming” the outer vertexes. The process of removing the terminal vertexes at each branch with its adjacent edge is a deformation retraction.
 - ii. A *star-like* digraph has a vertex v that connects to all other vertexes by linear digraphs. Such a graph is contractible to v , e.g., a facet $\sigma^{(2)}$ of a tetrahedron $\sigma^{(3)}$ can be contracted to its opposite vertex.
 - iii. A k -dimensional cube $I_n^k = I_n \times I_n \times \dots \times I_n$ (direct product of $k \geq 1$ I_n -lines), can be retracted to each of its facets, $I_n^k \simeq I_n^{k-1}$, and ultimately contracted.
 - iv. Cycling triangle and a cycling square are contractible. Longer cycles, $S_{n>4}$, loose contractibility: $H_1(S_{n>4}, \mathbb{K}) \cong \mathbb{K}$. Furthermore, two unequal cycles, $S_{n>4}$ and $S_{m>4}$, $n \neq m$, are homotopy inequivalent.
- If $r : G \rightarrow H$ is a deformation retraction, then G and H are homotopy equivalent and the map r is homotopy inverse of i and vice versa.
 - If a vertex v connects to a group of other vertexes, v_1, \dots, v_n , among which there is a special vertex, v_p , that connects to all the remaining v s whenever v does ($v \rightarrow v_i \implies v_p \rightarrow v_i$, then removing v along with all of its adjacent edges is a homology-preserving deformation retraction. This procedure may be viewed as removing this special kind of an “embedded star” from G . The arrows in this construction can be simultaneously reversed ($v \leftarrow v_i \implies v_p \leftarrow v_i$).

10. The topological complexity of a path-connected topological space X , $\text{TC}(X)$, is defined as the smallest number of open sets, U_1, U_2, \dots, U_k , required to cover $X \times X$, such that each set U_i allows for continuous motion planning from a starting to an ending point within its domain [93]. The value $\text{TC}(X)$ is a homotopy invariant [94], and for the spaces discussed above $\text{TC}(\mathcal{E}_1^{(2)}) = \text{TC}(\mathcal{E}_1^{(3)}) = \text{TC}(\mathcal{E}_1^{(4)}) = 2$.

VII. REFERENCES

- [1] Koch, C., Massimini, M., Boly, M. & Tononi, G. Neural correlates of consciousness: progress and problems. *Nat. Rev. Neurosci.* **17**(5): 307–321 (2016).
- [2] Dragoi, G. & Tonegawa, S. Preplay of future place cell sequences by hippocampal cellular assemblies. *Nature* **469**: 397–401 (2011).
- [3] Dragoi, G. & Tonegawa, S. Distinct preplay of multiple novel spatial experiences in the rat. *Proc. Natl. Acad. Sci.* **110**(22): 9100–5 (2013).
- [4] Carr, M., Jadhav, S. & Frank, L. Hippocampal replay in the awake state: a potential substrate for memory consolidation and retrieval. *Nat. Neurosci.* **14**: 147–153 (2011).
- [5] Chen, Z. & Wilson, M. How our understanding of memory replay evolves. *J Neurophys.* **129**(3): 552–580 (2023).
- [6] Liu, X., Ramirez, S., Pang, P., Puryear, C., Govindarajan, A., Deisseroth, K. & Tonegawa, S. Optogenetic stimulation of a hippocampal engram activates fear memory recall. *Nature* **484**(7394): 381–385 (2012).
- [7] Gridchyn, I., Schoenenberger, P., O’Neill, J. & Csicsvari, J. Assembly-Specific Disruption of Hippocampal Replay Leads to Selective Memory Deficit. *Neuron* **106**(2): 291–300.e6 (2020).
- [8] Knudsen, E. & Wallis, J. Hippocampal neurons construct a map of an abstract value space. *Cell*, **184**(18): 4640–4650.e10 (2021).
- [9] Kolibius, L., et al. Hippocampal neurons code individual episodic memories in humans. *Nat. Hum. Behav.* **7**(11): 1968–1979 (2023).
- [10] Wirth, S., Yanike, M., Frank, L., Smith, A., Brown, E. & Suzuki, W. Single neurons in the monkey hippocampus and learning of new associations. *Science* **300**(5625): 1578–1581 (2003).
- [11] Cao, R., Li, X., Brandmeir, N. & Wang, S. Encoding of facial features by single neurons in the human amygdala and hippocampus. *Comm. Biol.*, **4**(1): 1394 (2021).
- [12] Kutter, E., Bostroem, J., Elger, C., Mormann, F. & Nieder, A. Single Neurons in the Human Brain Encode Numbers. *Neuron* **100**(3): 753–761.e4 (2018).
- [13] Fortin N., Agster, K., & Eichenbaum, H. Critical role of the hippocampus in memory for sequences of events. *Nat Neurosci.* **5**: 458–462 (2002).
- [14] DuBrow, S. & Davachi, L. The influence of context boundaries on memory for the sequential order of events. *J. Exp. Psychol. Gen.* **142**: 1277–1286 (2013).
- [15] Davachi, L. & DuBrow, S. How the hippocampus preserves order: the role of prediction and context. *Trends Cogn. Sci.* **19**: 92–99.117 (2015).
- [16] Murray, E. & Baxter, M. Conditioned stimulus selectivity for familiar events and impaired ability to learn new stimulus sequences in monkeys with hippocampal lesions. *J Neurosci.* **26**(23): 6069–6082 (2006).
- [17] Henin, S., Turk-Browne, N., Friedman, D., Liu, A., Dugan, P., Flinker, A., Doyle, W., Devinsky, O. & Melloni, L. Learning hierarchical sequence representations across human cortex and hippocampus. *Sci. Adv.* **7**(8): eabc4530 (2021).
- [18] Friston, K. & Buzsáki, G. The functional anatomy of time: what and when in the brain. *Trends Cogn. Sci.* **20**: 500–511 (2016).
- [19] Hsieh, L., Gruber, M., Jenkins, L. & Ranganath, C. Hippocampal activity patterns carry information about objects in temporal context. *Neuron* **81**: 1165–1178 (2014).

- [20] Nielson, D.M. et al. Human hippocampus represents space and time during retrieval of real-world memories. *Proc. Natl. Acad. Sci.* **112**: 11078–11083 (2015).
- [21] Kyle, C. Stokes, J., Lieberman, J., Hassan, A. & Ekstrom, A. Successful retrieval of competing spatial environments involves hippocampal pattern separation mechanisms. *eLife* **4**: 1–19 (2015).
- [22] Nicolelis, M., Fanselow, E. & Ghazanfar, A. Hebb’s dream: the resurgence of cell assemblies. *Neuron* **19**(2): 219–221 (1997).
- [23] Tetzlaff, C., Dasgupta, S., Kulvicius, T. & Wörgötter, F. The Use of Hebbian Cell Assemblies for Nonlinear Computation. *Sci Rep.* **5**: 12866 (2015).
- [24] Buzsáki, G. Neural syntax: cell assemblies, synapsembles, and readers. *Neuron* **68**: 362–385 (2010).
- [25] Poucet, B. Spatial cognitive maps in animals: new hypotheses on their structure and neural mechanisms. *Psychol. Rev.* **100**: 163–182 (1993).
- [26] Terada, S., Sakurai, Y., Nakahara, H. & Fujisawa, S. Temporal and rate coding for discrete event sequences in the hippocampus. *Neuron* **94**: 1248–1262 (2017).
- [27] Maurer, A., Vanhoads, S., Sutherland, G., Lipa, P. & McNaughton, B. Self-motion and the origin of differential spatial scaling along the septo-temporal axis of the hippocampus. *Hippocampus* **15**, 841–852 (2005).
- [28] Mau, W., Sullivan, D., Kinsky, N., Hasselmo, M. Howard, M. & Eichenbaum, H. The same hippocampal CA1 population simultaneously codes temporal information over multiple timescales. *Curr. Biol.* **28**: 1–10 (2018).
- [29] Ezzyat, Y. & Davachi, L. Similarity breeds proximity: pattern similarity within and across contexts is related to later mnemonic judgments of temporal proximity. *Neuron* **81**: 1179–1189 (2014).
- [30] Gothard, K., Skaggs, W. & McNaughton B. Dynamics of mismatch correction in the hippocampal ensemble code for space: interaction between path integration and environmental cues. *J Neurosci.* **16**: 8027–8040 (1996).
- [31] Leutgeb, J., Leutgeb, S., Treves, A., Meyer, R., Barnes, C., McNaughton, B., Moser, M-B. & Moser, E. Progressive transformation of hippocampal neuronal representations in “morphed” environments. *Neuron* **48**: 345–358 (2005).
- [32] Wills, T., Lever, C., Cacucci, F., Burgess, N. & O’Keefe J. Attractor dynamics in the hippocampal representation of the local environment. *Science* **308**: 873–876 (2005).
- [33] Touretzky, D., Weisman, W., Fuhs, M., Skaggs, W., Fenton, A. & Muller, R. Deforming the hippocampal map. *Hippocampus* **15**: 41–55 (2005).
- [34] Place, R. & Nitz, D. Cognitive Maps: Distortions of the Hippocampal Space Map Define Neighborhoods. *Curr. Biol.* **30**: R340–R342 (2020).
- [35] Bellmund, J., de Cothi, W., Ruiter, T., Nau, M., Barry, C. & Doeller, C. Deforming the metric of cognitive maps distorts memory. *Nat. Hum Behav.* **4**: 177–188 (2020).
- [36] Dabaghian, Y., Brandt, V. & Frank, L. Reconceiving the hippocampal map as a topological template. *eLife* 2014;10.7554/eLife.03476 (2014).
- [37] Rueckemann, J., Sosa, M., Giocomo, L. & Buffalo, E. The grid code for ordered experience. *Nat Rev Neurosci.* **22**: 637–649 (2021).
- [38] Dabaghian, Y., Mémoli, F., Frank, L. & Carlsson, G. A Topological Paradigm for Hippocampal Spatial Map Formation Using Persistent Homology, *PLoS Comput. Biol.*, **8**: e1002581 (2012).
- [39] Curto, C. & Itskov, V. Cell groups reveal structure of stimulus space, *PLoS Comput. Biol.* **4**: e1000205 (2008).
- [40] Ghrist, R. Barcodes: The persistent topology of data, *Bull. Amer. Math. Soc.* **45**: 61–75 (2008).
- [41] Arai, M., Brandt, V. & Dabaghian Y. The effects of theta precession on spatial learning and simplicial complex dynamics in a topological model of the hippocampal spatial map. *PLoS Comput Biol.* **10**:

- e1003651 (2014).
- [42] Basso, E., Arai, M. & Dabaghian, Y. The effects of gamma synchronization on spatial learning in a topological model of the hippocampal spatial map. *PLoS Comput. Biol.* **12**: 9 (2016).
- [43] Hoffman, K., Babichev, A. & Dabaghian, Y. A model of topological mapping of space in bat hippocampus. *Hippocampus* **26**: 1345–1353 (2016).
- [44] Babichev, A., Mémoli, F., Ji, D. & Dabaghian, Y. A topological model of the hippocampal cell simplex network. *Front. Comput. Neurosci.*, **10**: 50 (2016).
- [45] Babichev, A. & Dabaghian, Y. Transient cell simplex networks encode stable spatial memories. *Sci. Rep.* **7**: 3959 (2017).
- [46] Dabaghian, Y. Through synapses to spatial memory maps: a topological model. *Sci. Reports* **9**: 572 (2018).
- [47] Dabaghian, Y. From Topological Analyses to Functional Modeling: The Case of Hippocampus. *Front. Comput. Neurosci.* **14** (2021).
- [48] Kang, L., Xu, B. & Morozov, D. Evaluating State Space Discovery by Persistent Cohomology in the Spatial Representation System. *Front. Comput. Neurosci.* **15**(28): 616748 (2021).
- [49] Babichev, A., Morozov, D. & Dabaghian, Y. Replays of spatial memories suppress topological fluctuations in cognitive map. *Network Neuroscience* **3**(3): 707-724 (2019).
- [50] Babichev, A., Morozov, D. & Dabaghian, Y. Robust spatial memory maps encoded by networks with transient connections. *PLoS Comput. Bio.* **14**(9): e1006433 (2018).
- [51] Smith, B. Topological Foundations of Cognitive Science. In: Eschenbach, C., et al. (eds.): Graduiertenkolleg Kognitionswissenschaft, Hamburg, Rep. 37, Buffalo, NY, pp. 3-22 (1994).
- [52] Dabaghian, Y., Cohn, A. G. & Frank, L. Topological maps from signals. In: *Proceedings of the 15th annual ACM symposium GIS '07*, Article 61, 1–4 New York, NY (2007).
- [53] Grigor'yan, A., Muranov, Y. & Jimenez, R. Homology of Digraphs. *Math Notes* **109**: 712–726 (2021).
- [54] Grigor'yan, A., Lin, Y., Muranov, Y. & Yau, Sh-T. Path Complexes and their Homologies. *J Math Sci.* **248**: 564–599 (2020).
- [55] Grigor'yan A., Muranov Y. & Yau Sh.-T. Graphs associated with simplicial complexes. *Homology, Homotopy Appl.* **16**: 295-311 (2014).
- [56] Grigor'yan A., Muranov Y. & Yau Sh.-T. On a cohomology of digraphs and Hochschild cohomology. *J Homotopy & Rel. Struct.* **11**(2): 209-230 (2016).
- [57] Grigor'yan A., Lin, Y., Muranov Yu. & Yau Sh.-T. Homotopy Theory for Digraphs, *Pure & Appl. Math. Quarterly* **10**(4): 619–674 (2014).
- [58] G. Buzsáki, *Rhythms in the brain*. Oxford University Press, USA (2011).
- [59] Alexandrov, P. *Elementary concepts of topology*. New York: F. Ungar Pub. (1965).
- [60] Edelsbrunner, H. & Harer, J. *Computational topology: an introduction*. Amer. Math. Soc. (2010).
- [61] Zomorodian, A. *Topology for Computing* Cambridge University Press, New York (2009).
- [62] Brown, E., Frank, L., Tang, D., Quirk, M. & Wilson, M. A statistical paradigm for neural spike train decoding applied to position prediction from ensemble firing patterns of rat hippocampal place cells. *J. Neurosci.* **18**: 7411-7425 (1998).
- [63] Jensen, O. & Lisman, J.E. Position reconstruction from an ensemble of hippocampal place cells: contribution of theta phase coding. *J. Neurophys.* **83**: 2602-2609 (2000).
- [64] Guger, C., Gener, T., Pennartz, C., Brotons-Mas, J., Edlinger, G., Bermúdez, I., Badia, S., Verschure, P., Schaffelhofer, S. & Sanchez-Vives M. Real-time position reconstruction with hippocampal place cells. *Front. Neurosci.*, **5**: 85 (2011).
- [65] Akhtiamov, D., Cohn, A. G. & Dabaghian, Y. Spatial representability of neuronal activity. *Sci. Reps.*

- 11**: 20957 (2021).
- [66] Tancer, M. Intersection Patterns of Convex Sets via Simplicial Complexes: A Survey. In: Pach J, Ed. *Thirty Essays on Geometric Graph Theory*: Springer New York. pp. 521-40 (2013).
- [67] Muller, R., Stead, M., Pach, J. The hippocampus as a cognitive graph. *J. Gen. Physiol.* **107**: 663-694 (1996).
- [68] Trullier, O. & Meyer, J-A. Animat navigation using a cognitive graph, *Biol. Cybern.* **83**: 271-285 (2000).
- [69] Chrastil, R., Warren, W. From Cognitive Maps to Cognitive Graphs, *PLoS One* **9**: e112544 (2014).
- [70] Burgess, N. & O'Keefe, J. Cognitive graphs, resistive grids, and the hippocampal representation of space. *J. Gen. Physiol.* **107**: 659-662 (1996).
- [71] Peer, M., Brunec, I., Newcombe, N., & Epstein, R. Structuring Knowledge with Cognitive Maps and Cognitive Graphs. *Trends Cog. Sci.*, **25**(1): 37–54 (2021).
- [72] Ericson, J. & Warren, W. Probing the invariant structure of spatial knowledge: Support for the cognitive graph hypothesis. *Cognition*, **200**: 104276 (2020).
- [73] Farzanfar, D., Spiers, H., Moscovitch, M. & Rosenbaum, R. From cognitive maps to spatial schemas. *Nat. Rev. Neurosci.* **24**: 63–79 (2023).
- [74] Ólafsdóttir, H., Bush, D. & Barry, C. The Role of Hippocampal Replay in Memory and Planning. *Curr Biol.* **28**(1): R37-R50 (2018).
- [75] Farooq, U., Sibille, J., Liu, K. & Dragoi, G. Strengthened Temporal Coordination within Pre-existing Sequential Cell Assemblies Supports Trajectory Replay. *Neuron* **103**(4): 719–733.e7 (2019).
- [76] Dragoi G. The generative grammar of the brain: a critique of internally generated representations. *Nat. Rev. Neurosci.* **25**(1): 60–75 (2024).
- [77] Vaz, A., Wittig, J., Inati, S. & Zaghoul, K. Backbone spiking sequence as a basis for preplay, replay, and default states in human cortex. *Nat Commun* **14**: 4723 (2023).
- [78] Bertram, R., Butte, M., Kiemel, T. & Sherman, A. Topological and phenomenological classification of bursting oscillations. *Bull. Math. Bio.* **57**: 413–439 (1995).
- [79] Izhikevich, E. Neural Excitability, Spiking, and Bursting. *Int J Bifurc & Chaos.* **10**(06): 1171-266 (2000).
- [80] Wu, X. & Foster, D. Hippocampal Replay Captures the Unique Topological Structure of a Novel Environment. *J Neurosci.* **34**: 6459-6469 (2014).
- [81] Poucet, B. & Herrmann, T. Exploratory patterns of rats on a complex maze provide evidence for topological coding. *Behav Processes* **53**: 155-162 (2001).
- [82] Alvernhe, A., Sargolini, F. & Poucet, B. Rats build and update topological representations through exploration. *Anim. Cogn.* **15**: 359-368 (2012).
- [83] Goodrich-Hunsaker, N., Howard, B., Hunsaker, M. & Kesner, R. Human topological task adapted for rats: Spatial information processes of the parietal cortex. *Neurobiol Learn & Mem.* **90**: 389-394 (2008).
- [84] Chen, Z., Gomperts, S., Yamamoto, J. & Wilson, M. Neural representation of spatial topology in the rodent hippocampus. *Neural Comput* **26**: 1-39 (2014).
- [85] Alvernhe, A., Van Cauter, T., Save, E. & Poucet, B. Different CA1 and CA3 representations of novel routes in a shortcut situation. *J Neurosci.* **28**(29): 7324-7333 (2008).
- [86] Alvernhe, A., Save, E. & Poucet, B. Local remapping of place cell firing in the Tolman detour task. *Eur. J. Neurosci.* **33**(9): 1696-1705 (2011).
- [87] Wei, X. & Wei, G.-W. Persistent Topological Laplacians—A Survey. *Mathematics*, **13**(2): 208 (2025).
- [88] Chaplin, T., Harrington, H. & Tillmann, U. Grounded Persistent Path Homology: A Stable, Topolog-

- ical Descriptor for Weighted Digraphs. *Found Comput Math* 10.1007/s10208-024-09679-2 (2024).
- [89] Hafting, T., Fyhn, M., Molden, S., Moser, M.-B. & Moser, E. Microstructure of a spatial map in the entorhinal cortex. *Nature* **436**: 801–806 (2005).
- [90] Brun, V., Solstad, T., Kjelstrup, K., Fyhn, M., Witter, M., Moser, E. & Moser, M.-B. Progressive increase in grid scale from dorsal to ventral medial entorhinal cortex. *Hippocampus* **18**(12): 1200-12 (2008).
- [91] Chaplin, T. First Betti number of the path homology of random directed graphs. *J Appl. & Comput. Topology* **8**: 1503–1549 (2024).
- [92] Yartsev, M. & Ulanovsky, N. Representation of Three-Dimensional Space in the Hippocampus of Flying Bats. *Science* **340**: 367-372 (2013).
- [93] Farber, M. Topological Complexity of Motion Planning. *Discrete & Comput. Geom.* **29**: 211–221 (2003).
- [94] Schwarz, A. The genus of a fiber space, *Dokl. Akad. Nauk SSSR* **119**(2): 219–222 (1958).
- [95] Eichenbaum, H., Dudchenko, P., Wood, E., Shapiro, M. & Tanila, H. The hippocampus, memory, and place cells: is it spatial memory or a memory space? *Neuron* **23**: 209-226 (1999).
- [96] Crystal, J. Episodic-like memory in animals. *Behav. Brain Res.* **215**(2): 235-43 (2010).
- [97] Eichenbaum, H. On the integration of space, time, and memory. *Neuron* **95**: 1007–1018 (2017).
- [98] Lisman, J. Buzsáki, G., Eichenbaum, H., Nadel, L., Ranganath, C. & Redish, A. Viewpoints: how the hippocampus contributes to memory, navigation and cognition. *Nat. Neurosci.* **20**: 1434-48 (2017).
- [99] Deuker, L., Bellmund, J., Navarro Schröder, T. & Doeller, C. An event map of memory space in the hippocampus. *eLife* **5**: 1–26 (2016).
- [100] Liu, C., Todorova, R., Tang, W., Oliva, A. & Fernandez-Ruiz, A. Associative and predictive hippocampal codes support memory-guided behaviors. *Science*, **382**(6668): eadi8237 (2023).
- [101] Babichev, A. & Dabaghian, Y. Topological schemas of memory spaces. *Front. Comput. Neurosci.* **12**, 10.3389/fncom.2018.00027 (2018).
- [102] O’Keefe, J. & Nadel, L. *The hippocampus as a cognitive map*. Oxford University Press (1978).
- [103] Grieves, R. & Jeffery, K. The representation of space in the brain. *Behav. Processes.* **135**: 113-31 (2017).
- [104] Moser, E., Kropff, E. & Moser M.-B. Place Cells, Grid Cells, and the Brain’s Spatial Representation System. *Annu. Rev. Neurosci.* **31**(1): 69-89 (2008).
- [105] McCord. M. Singular homology groups and homotopy groups of finite topological spaces. *Duke Math J* **33**: 465–474 (1966).
- [106] Alexandroff P. Diskrete Räume, *Recueil Mathématique (Mat. Sbornik)* **2**(44): 501-518 (1937).
- [107] El-Fattah El-Atik, A., Abd El-Monsef, M., Lashin, E. On finite T_0 topological spaces, *Proceedings of the Ninth Prague Topological Symposium*: 75–90 (2001).
- [108] Stong, R. Finite topological spaces. *Trans Amer Math Soc* **123**: 325-340 (1966).
- [109] Osaki, T. Reduction of Finite Topological Spaces. *Interdisc. Inf. Sci* **5**: 149-155 (1999).
- [110] Shiraki, M. On finite topological spaces. *Rep. Sci. Kagoshima Univ.*, **1**: 1-8 (1968), **2**: 1-15 (1969).
- [111] Reimann, M., Nolte, M., Scolamiero, M., Turner, K., Perin, R., Chindemi, G., Dlotko, P., Levi, R., Hess, K. & Markram, H. Cliques of Neurons Bound into Cavities Provide a Missing Link between Structure and Function. *Front. Comput. Neurosci.* **11**: 48 (2017).
- [112] Parra-Barrero, E., Vijayabaskaran, S., Seabrook, E., Wiskott, L. & Cheng, S. A map of spatial navigation for neuroscience. *Neurosci & Biobehav Rev.* **152**: 105200 (2023).
- [113] Balaguer, J., Spiers, H., Hassabis, D. & Summerfield, C. Neural Mechanisms of Hierarchical Planning in a Virtual Subway Network. *Neuron* **90**(4): 893–903 (2016).
- [114] Audrain, S. & McAndrews, M. Schemas provide a scaffold for neocortical integration of new mem-

- ories over time. *Nat Commun* **13**: 5795 (2022).
- [115] Winocur, G. & Moscovitch, M. Memory Transformation and Systems Consolidation. *J Int. Neuropsych. Soc.* **17**(5): 766-780 (2011).
- [116] Preston, A. & Eichenbaum, H. Interplay of Hippocampus and Prefrontal Cortex in Memory. *Current Biology* **23**(17): R764-R773 (2013).
- [117] Sekeres, M., Winocur, G. & Moscovitch, M. The hippocampus and related neocortical structures in memory transformation. *Neurosci. Lett.* **680**: 39–53 (2018).
- [118] Robin, J. & Moscovitch, M. Details, gist and schema: Hippocampal–neocortical interactions underlying recent and remote episodic and spatial memory. *Curr. Opin. Behav. Sci.* **17**: 114–123 (2017).
- [119] Sekeres, M. J. et al. Changes in patterns of neural activity underlie a time-dependent transformation of memory in rats and humans. *Hippocampus* **28**: 745–764 (2018).
- [120] Squire, L., Genzel, L., Wixted, J. & Morris, R. Memory consolidation. *Cold Spring Harb. Perspect. Biol.* **7**: 1–22 (2015).
- [121] O’Reilly, R. & Rudy, J. Computational principles of learning in the neocortex and hippocampus. *Hippocampus* **10**(4): 389-397 (2000).
- [122] Benna, M. & Fusi, S. Computational principles of synaptic memory consolidation. *Nat. Neurosci.* **19**(12): 1697-1706 (2016).
- [123] Tse, D., Langston, R., Kakeyama, M., Bethus, I., Spooner, P., Wood, E., Witter, M. & Morris, R. Schemas and Memory Consolidation. *Science* **316**: 76-82 (2007).
- [124] Tse, D., Langston, R., Bethus, I., Wood, E., Witter, M., et al. Does assimilation into schemas involve systems or cellular consolidation? It’s not just time. *Neurobiol Learn & Mem* **89**: 361-365 (2008).
- [125] Morris, R. Elements of a neurobiological theory of hippocampal function: the role of synaptic plasticity, synaptic tagging and schemas. *Eur. J Neurosci.* **23**: 2829-2846 (2006).
- [126] Babichev, A., Cheng, S. & Dabaghian, Y. Topological schemas of cognitive maps and spatial learning. *Front. Comput. Neurosci.* **10**: 18 (2016).
- [127] Buzsáki, G. & Tingley, D. Space and Time: The Hippocampus as a Sequence Generator. *Trends Cog. Sci.* **22**(10): 853–869 (2018).
- [128] Deng, X., Chen, S., Sosa, M., Karlsson, M., Wei, X. & Frank, L. A Variable Clock Underlies Internally Generated Hippocampal Sequences. *J Neurosci.* **42**(18): 3797–3810 (2022).
- [129] Sosa, M., Plitt, M. & Giocomo, L. Hippocampal sequences span experience relative to rewards. *bioRxiv* 2023.12.27.573490 (2023).
- [130] McKenzie, S. & Eichenbaum, H. Consolidation and reconsolidation: two lives of memories? *Neuron* **71**(2): 224–233 (2011).
- [131] Raju, R., Guntupalli, J., Zhou, G., Wendelken, C., Lázaro-Gredilla, M. & George, D. Space is a latent sequence: A theory of the hippocampus. *Sci. Adv.* **10**(31): eadm8470 (2024).
- [132] Rabson, D., Huesman, J. & Fisher, B. Cohomology for Anyone. *Found. Phys.* **33**(12): 1769-96 (2003)
- [133] Stasheff, J. A survey of cohomological physics. nLab (1999).
- [134] Yiu, Y-H., Leutgeb, J. & Leibold, C. Directional Tuning of Phase Precession Properties in the Hippocampus. *J Neurosci.* **42**(11): 2282–2297 (2022).
- [135] Chowdhury, S., Huntsman, S. & Yutin, M. Path Homology and Temporal Networks. In: Benito, R., Cherifi, C. et al. (eds) *Complex Networks & Their Applications IX*. Vol 944. Springer, Cham (2021).
- [136] Knill, O. The energy of a simplicial complex. *Lin Alg. & Appl.* **600**: 96-129 (2020).
- [137] Ivashchenko, A. Contractible transformations do not change the homology groups of graphs. *Discrete Math.* **126**: 159–170 (1994).